Credit : ESA and the *Planck* Collaboration

Removal and marginalisation of “well-known” foregrounds

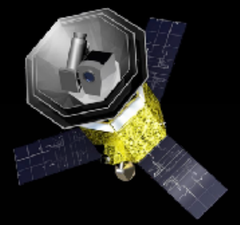

Benjamin Beringue
Postdoc @ APC-CNRS
February, 9th 2026

CosmoForward workshop

SciPol

erc

cnrs

Science from the large scale cosmic microwave background polarization structure

Outline

- Foreground contamination of CMB observables
- Modelling of small scales temperature and polarisation anistropies
- Component separation methods

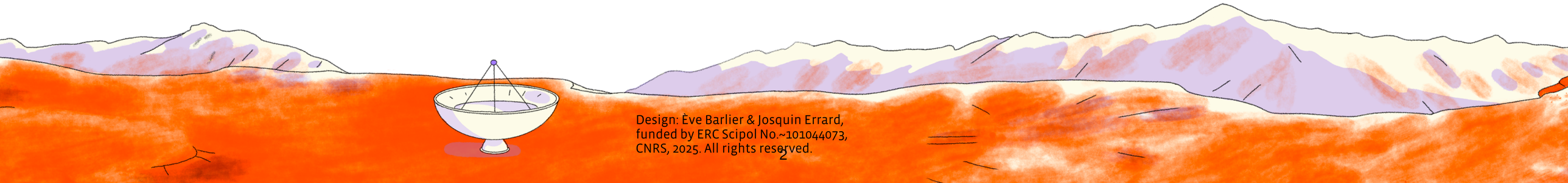

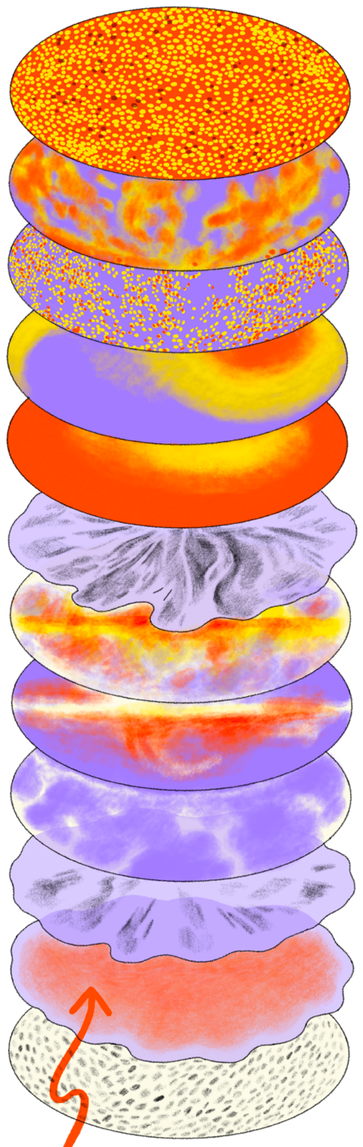

B-modes

E-modes

Intensity anisotropies

Dipole

Monopole

CMB

Gravitational lensing

Galactic and extra-galactic foregrounds

Atmosphere

Systematics

Ground emissions

Noise

Foregrounds contamination

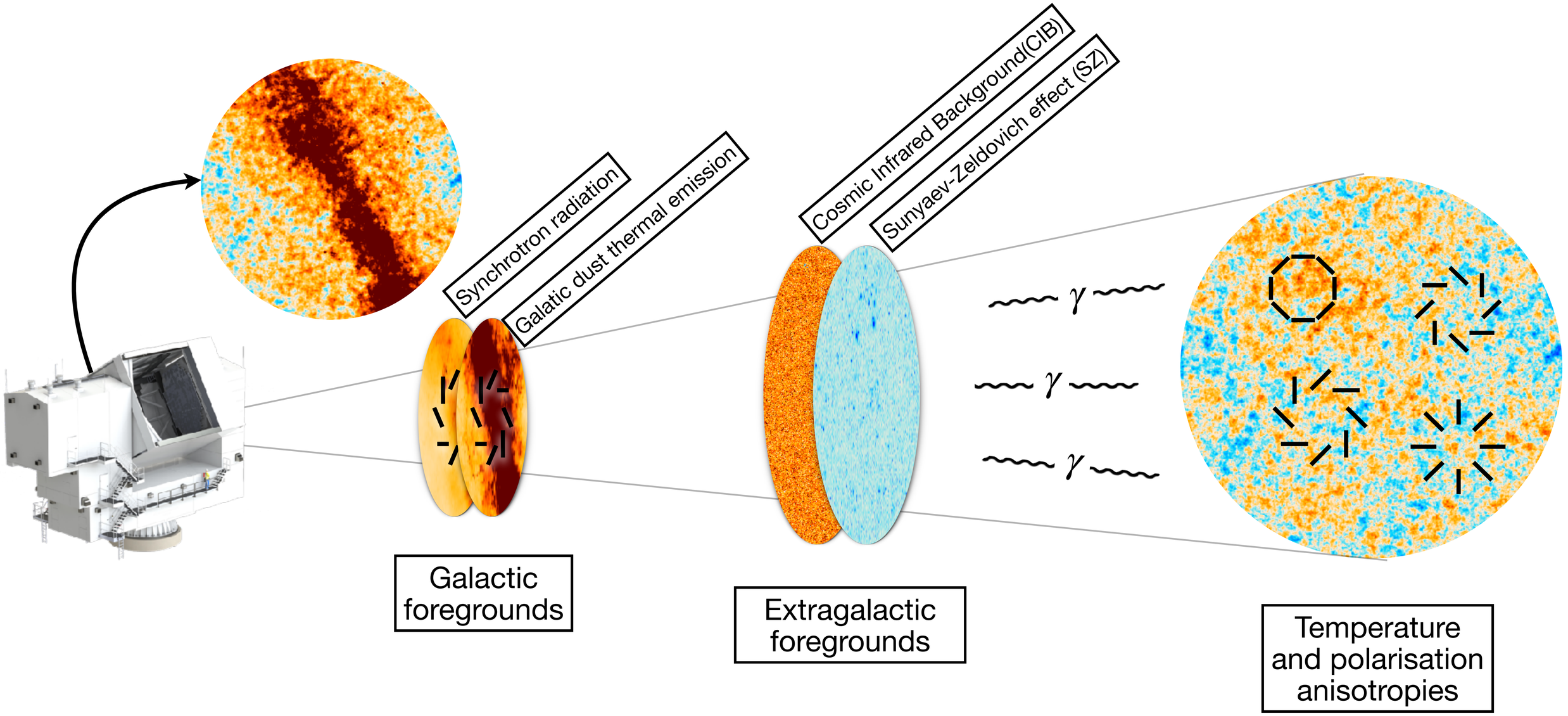

Foregrounds contamination

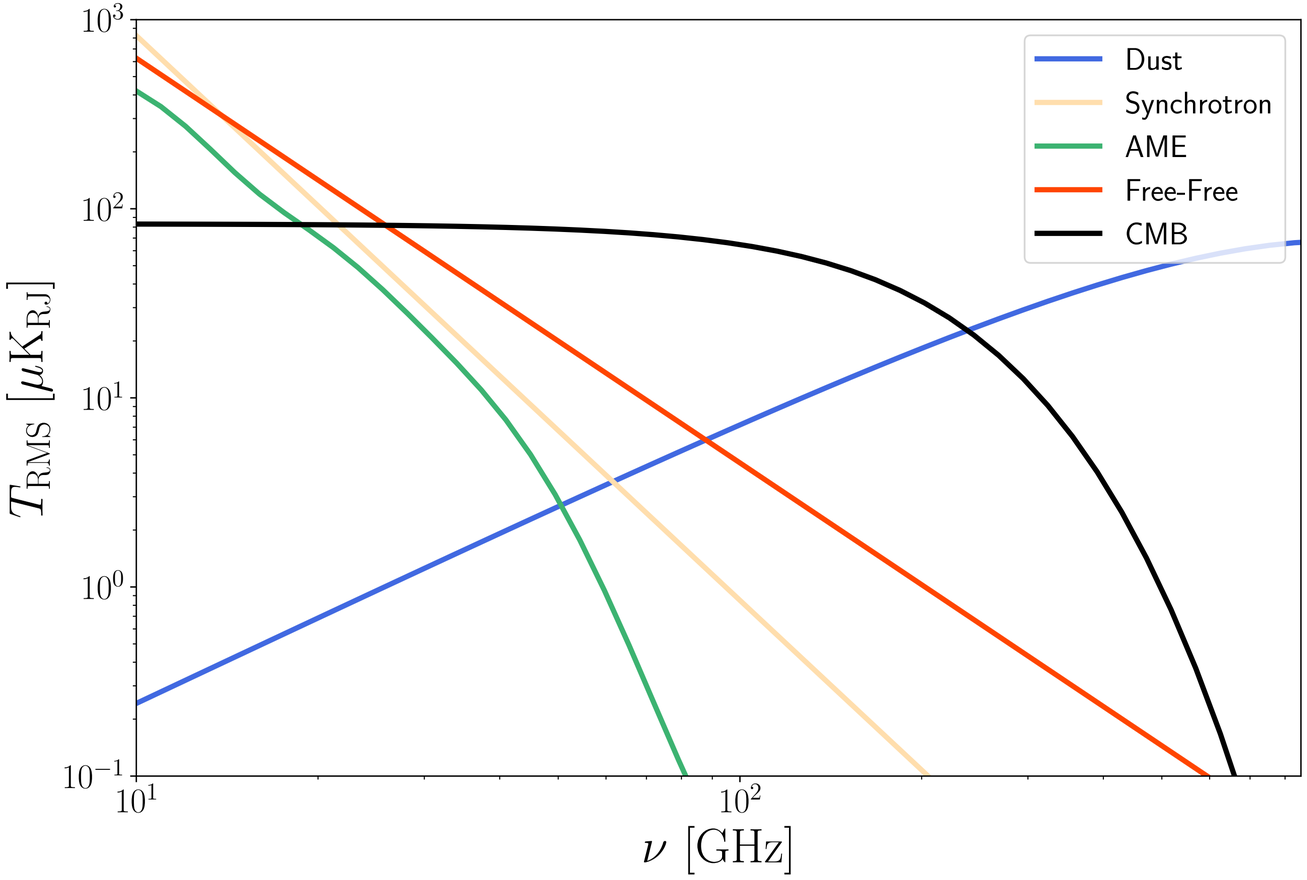

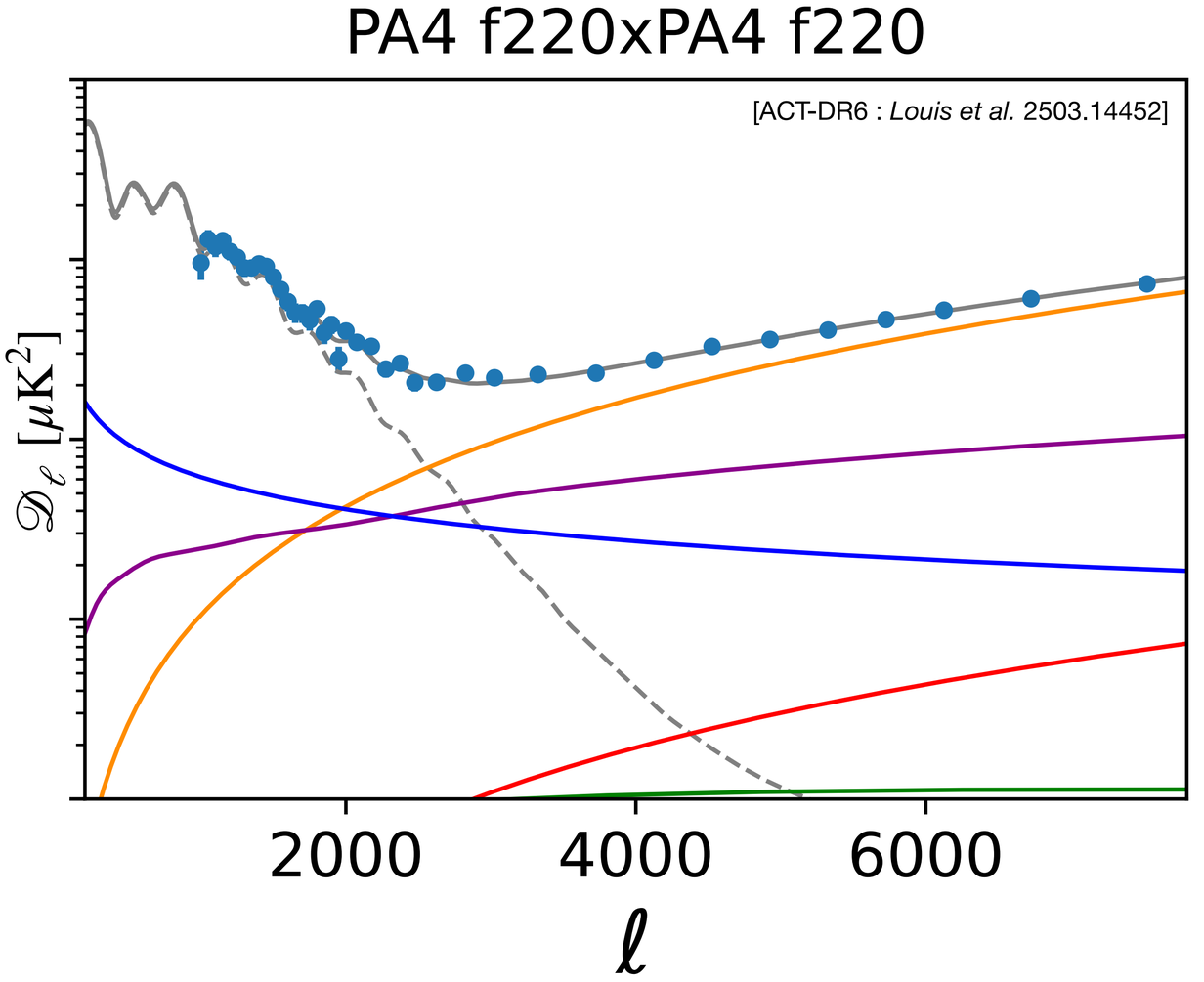

Outline

- Foreground contamination of CMB observables
- Modelling of small scales temperature and polarisation anistropies
- Component separation methods

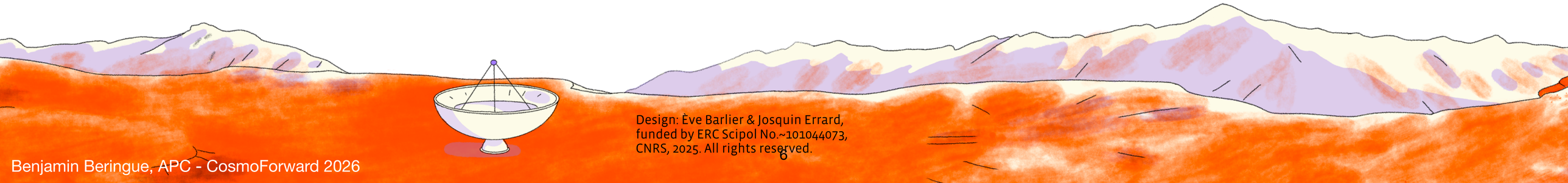

Modelling of small scales anisotropies - ACT-DR6

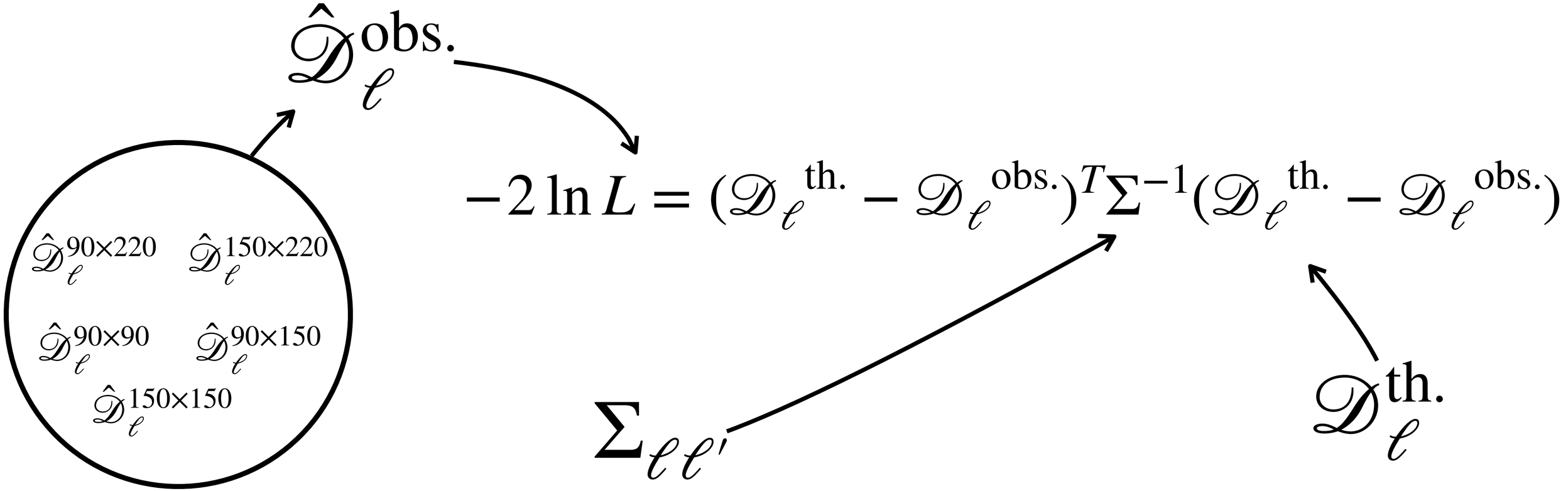

Modelling of small scales anisotropies - ACT-DR6

$$\mathscr{D}_\ell^{\text{th.}} = \mathscr{D}_\ell^{\text{CMB}} + \mathscr{D}_\ell^{\text{foregrounds}}$$

Modelling of small scales anisotropies - ACT-DR6

$$\mathscr{D}_\ell^{\mathrm{fgs.,TT}} = \mathscr{D}_\ell^{\mathrm{tSZ}} + \mathscr{D}_\ell^{\mathrm{kSZ}} + \mathscr{D}_\ell^{\mathrm{CIB-c}} + \mathscr{D}_\ell^{\mathrm{CIB-p}} + \mathscr{D}_\ell^{\mathrm{tSZ\times CIB}} + \mathscr{D}_\ell^{\mathrm{radio,TT}} + \mathscr{D}_\ell^{\mathrm{dust,TT}}$$

Modelling of small scales anisotropies - ACT-DR6

$$\mathscr{D}_\ell^{\rm fgs.,TT} = \mathscr{D}_\ell^{\rm tSZ} + \mathscr{D}_\ell^{\rm kSZ} + \mathscr{D}_\ell^{\rm CIB-c} + \mathscr{D}_\ell^{\rm CIB-p} + \mathscr{D}_\ell^{\rm tSZ\times CIB} + \mathscr{D}_\ell^{\rm radio,TT} + \mathscr{D}_\ell^{\rm dust,TT}$$

Thermal Sunyaev-Zel'dovich effect

- Inverse Compton Scattering of CMB photons by hot electrons in clusters

$$\mathscr{D}^{T_iT_j}_{\ell,\rm tSZ} = a_{\rm tSZ}\mathscr{D}^{\rm tSZ}_{\ell,\ell_0}\left[\frac{\ell}{\ell_0}\right]^{\alpha_{\rm tSZ}}\frac{f_{\rm tSZ}(\nu_i)f_{\rm tSZ}(\nu_j)}{f^2_{\rm tSZ}(\nu_0)}$$

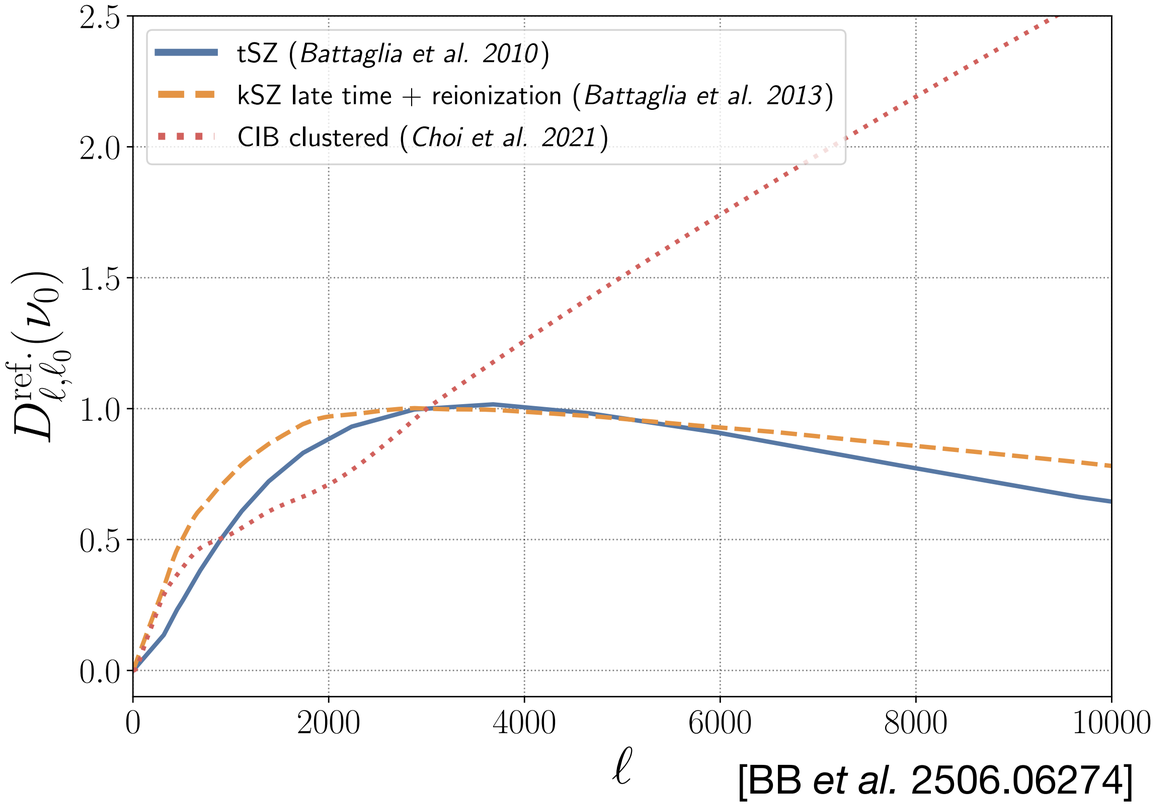

[BB *et al.* 2506.06274]

Modelling of small scales anisotropies - ACT-DR6

$$\mathscr{D}_\ell^{\text{fgs.,TT}} = \mathscr{D}_\ell^{\text{tSZ}} + \mathscr{D}_\ell^{\text{kSZ}} + \mathscr{D}_\ell^{\text{CIB-c}} + \mathscr{D}_\ell^{\text{CIB-p}} + \mathscr{D}_\ell^{\text{tSZ}\times\text{CIB}} + \mathscr{D}_\ell^{\text{radio,TT}} + \mathscr{D}_\ell^{\text{dust,TT}}$$

Kinetic Sunyaev-Zel'dovich effect

- Inverse Compton Scattering of CMB photons by hot electrons in clusters with peculiar velocity

$$\mathscr{D}^{T_iT_j}_{\ell,\text{kSZ}} = a_{\text{kSZ}}\mathscr{D}^{\text{kSZ}}_{\ell,\ell_0}$$

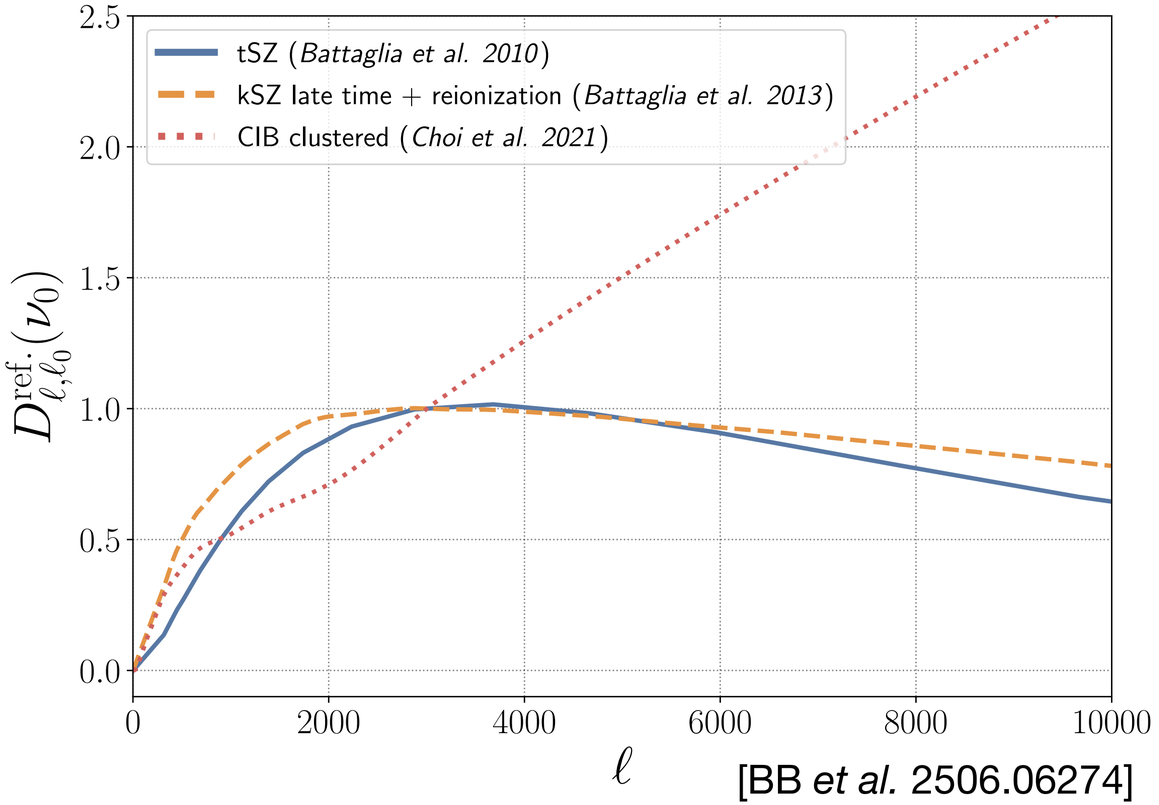

[BB *et al.* 2506.06274]

Modelling of small scales anisotropies - ACT-DR6

$$\mathscr{D}_\ell^{\rm fgs.,TT} = \mathscr{D}_\ell^{\rm tSZ} + \mathscr{D}_\ell^{\rm kSZ} + \mathscr{D}_\ell^{\rm CIB-c} + \mathscr{D}_\ell^{\rm CIB-p} + \mathscr{D}_\ell^{\rm tSZ\times CIB} + \mathscr{D}_\ell^{\rm radio,TT} + \mathscr{D}_\ell^{\rm dust,TT}$$

Clustered Cosmic Infrared Background

- Redshifted thermal dust emission from distant galaxies.

$$\mathscr{D}^{T_iT_j}_{\ell,\rm CIB-c} = a_c \mathscr{D}^{\rm CIB-c}_{\ell,\ell_0} \frac{\mu(\nu_i;\beta_c,T_d)\mu(\nu_j;\beta_c,T_d)}{\mu^2(\nu_0;\beta_c,T_d)}$$

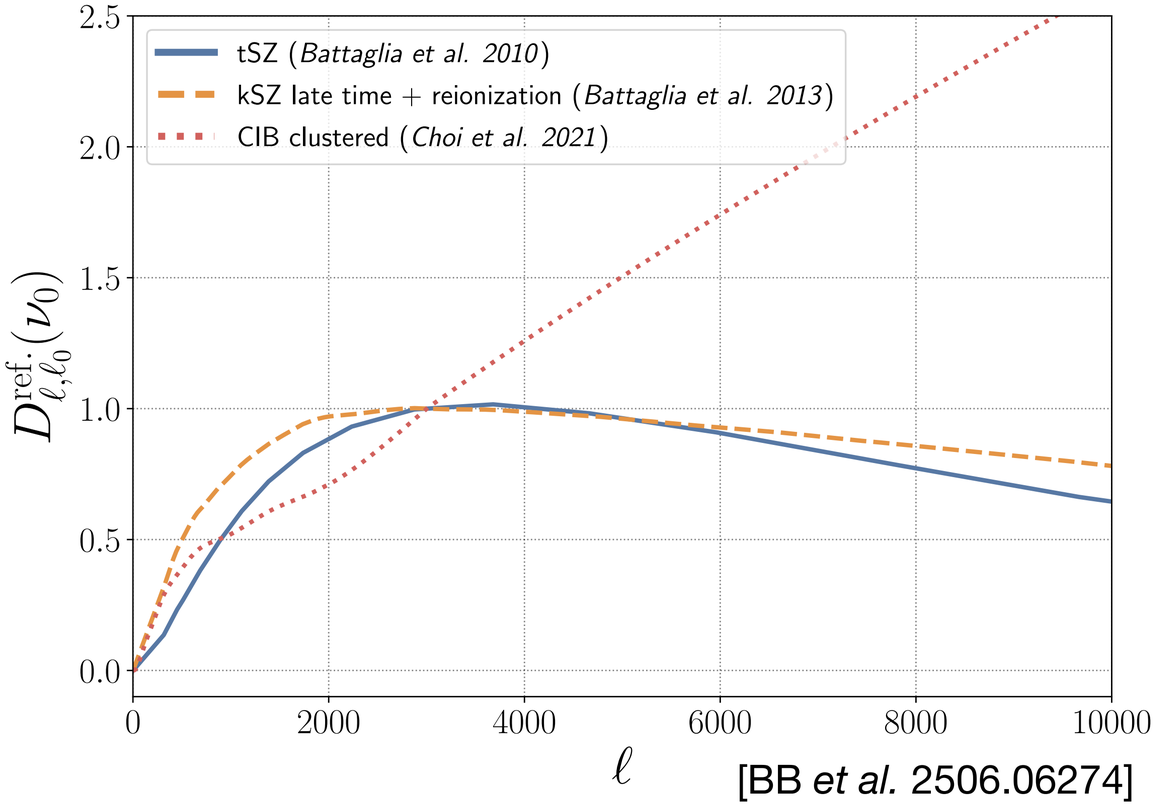

[BB *et al.* 2506.06274]

Modelling of small scales anisotropies - ACT-DR6

$$\mathscr{D}_\ell^{\rm fgs.,TT} = \mathscr{D}_\ell^{\rm tSZ} + \mathscr{D}_\ell^{\rm kSZ} + \mathscr{D}_\ell^{\rm CIB-c} + \mathscr{D}_\ell^{\rm CIB-p} + \mathscr{D}_\ell^{\rm tSZ\times CIB} + \mathscr{D}_\ell^{\rm radio,TT} + \mathscr{D}_\ell^{\rm dust,TT}$$

Poisson Cosmic Infrared Background

- Redshifted thermal dust emission from distant galaxies.

$$\mathscr{D}^{T_iT_j}_{\ell,\rm CIB-p} = a_p \left[\frac{\ell(\ell+1)}{\ell_0(\ell_0+1)}\right] \frac{\mu(\nu_i;\beta_p,T_d)\mu(\nu_j;\beta_p,T_d)}{\mu^2(\nu_0;\beta_p,T_d)}$$

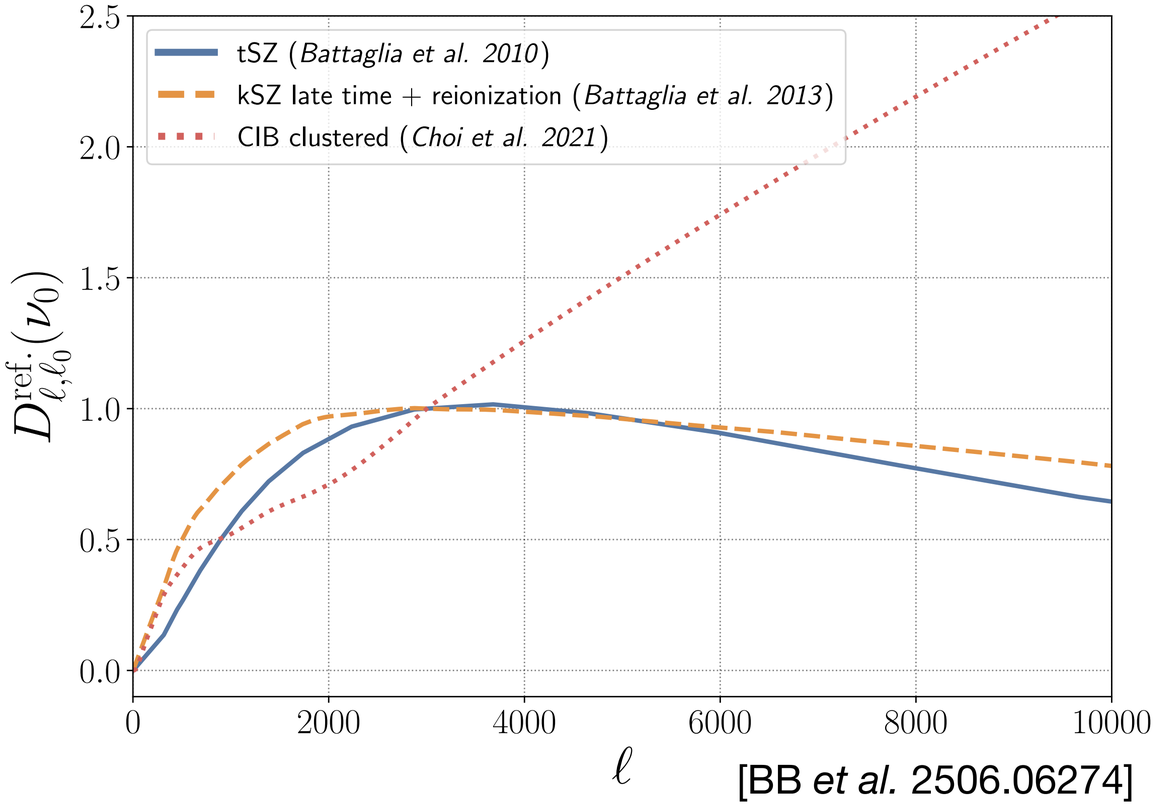

[BB *et al.* 2506.06274]

Modelling of small scales anisotropies - ACT-DR6

$$\mathscr{D}_\ell^{\text{fgs.,TT}} = \mathscr{D}_\ell^{\text{tSZ}} + \mathscr{D}_\ell^{\text{kSZ}} + \mathscr{D}_\ell^{\text{CIB-c}} + \mathscr{D}_\ell^{\text{CIB-p}} + \mathscr{D}_\ell^{\text{tSZ}\times\text{CIB}} + \mathscr{D}_\ell^{\text{radio,TT}} + \mathscr{D}_\ell^{\text{dust,TT}}$$

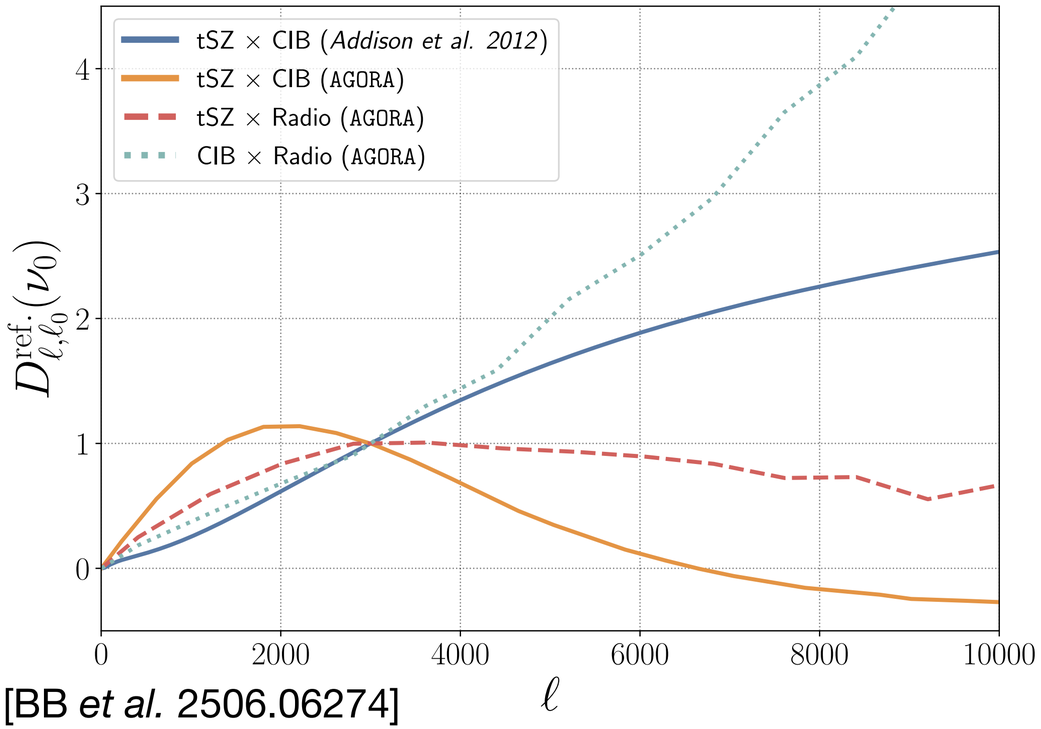

[BB *et al.* 2506.06274]

CIBxtSZ correlation

- tSZ and clustered CIB are sourced by the same clusters

$$\mathscr{D}^{T_iT_j}_{\ell,\text{tSZ}\times\text{CIB}} = -\xi_{yc}\sqrt{a_c a_{\text{tSZ}}}\,\mathscr{D}^{\text{tSZ}\times\text{CIB}}_{\ell,\ell_0} \times \left(\frac{f_{\text{tSZ}}(\nu_i)\mu(\nu_j;\beta_c,T_d) + f_{\text{tSZ}}(\nu_j)\mu(\nu_i;\beta_c,T_d)}{f_{\text{tSZ}}(\nu_0)\mu(\nu_0;\beta_c,T_d)}\right)$$

Modelling of small scales anisotropies - ACT-DR6

$$\mathscr{D}_\ell^{\text{fgs.,TT}} = \mathscr{D}_\ell^{\text{tSZ}} + \mathscr{D}_\ell^{\text{kSZ}} + \mathscr{D}_\ell^{\text{CIB-c}} + \mathscr{D}_\ell^{\text{CIB-p}} + \mathscr{D}_\ell^{\text{tSZ}\times\text{CIB}} + \mathscr{D}_\ell^{\text{radio,TT}} + \mathscr{D}_\ell^{\text{dust,TT}}$$

Poisson distributed Radio Galaxies

- Synchrotron emission from distant radio galaxies

$$\mathscr{D}^{X_i Y_j}_{\ell,\text{radio}} = a_{\text{s}}^{XY} \left[\frac{\ell(\ell+1)}{\ell_0(\ell_0+1)}\right] \left[\frac{g(\nu_i)g(\nu_j)}{g^2(\nu_0)}\right] \left[\frac{\nu_i\nu_j}{\nu_0^2}\right]^{\beta_s+2}$$

Modelling of small scales anisotropies - ACT-DR6

$$\mathscr{D}_\ell^{\text{fgs.,TT}} = \mathscr{D}_\ell^{\text{tSZ}} + \mathscr{D}_\ell^{\text{kSZ}} + \mathscr{D}_\ell^{\text{CIB-c}} + \mathscr{D}_\ell^{\text{CIB-p}} + \mathscr{D}_\ell^{\text{tSZ}\times\text{CIB}} + \mathscr{D}_\ell^{\text{radio,TT}} + \mathscr{D}_\ell^{\text{dust,TT}}$$

Residual galactic dust emission

- Thermal emission from galactic dust in the ACT footprint

$$\mathscr{D}_{\ell,g}^{T_iT_j} = a_g^{TT} \left[\frac{\ell}{\ell_0}\right]^{\alpha_g^{TT}} \frac{\mu(\nu_i;\beta_d,T_d^{\text{eff}})\mu(\nu_j;\beta_d,T_d^{\text{eff}})}{\mu^2(\nu_0;\beta_d,T_d^{\text{eff}})}$$

Modelling of small scales anisotropies - ACT-DR6

$$\mathscr{D}_\ell^{\text{fgs.,TT}} = \mathscr{D}_\ell^{\text{tSZ}} + \mathscr{D}_\ell^{\text{kSZ}} + \mathscr{D}_\ell^{\text{CIB}-\text{c}} + \mathscr{D}_\ell^{\text{CIB}-\text{p}} + \mathscr{D}_\ell^{\text{tSZ}\times\text{CIB}} + \mathscr{D}_\ell^{\text{radio,TT}} + \mathscr{D}_\ell^{\text{dust,TT}}$$

$$\mathscr{D}_\ell^{\text{fgs.,EE}} = \mathscr{D}_\ell^{\text{radio,EE}} + \mathscr{D}_\ell^{\text{dust,EE}}$$

$$\mathscr{D}_\ell^{\text{fgs.,TE}} = \mathscr{D}_\ell^{\text{radio,TE}} + \mathscr{D}_\ell^{\text{dust,TE}}$$

14 parameters

[BB *et al.* 2506.06274]

ACT-DR6 foreground modelling

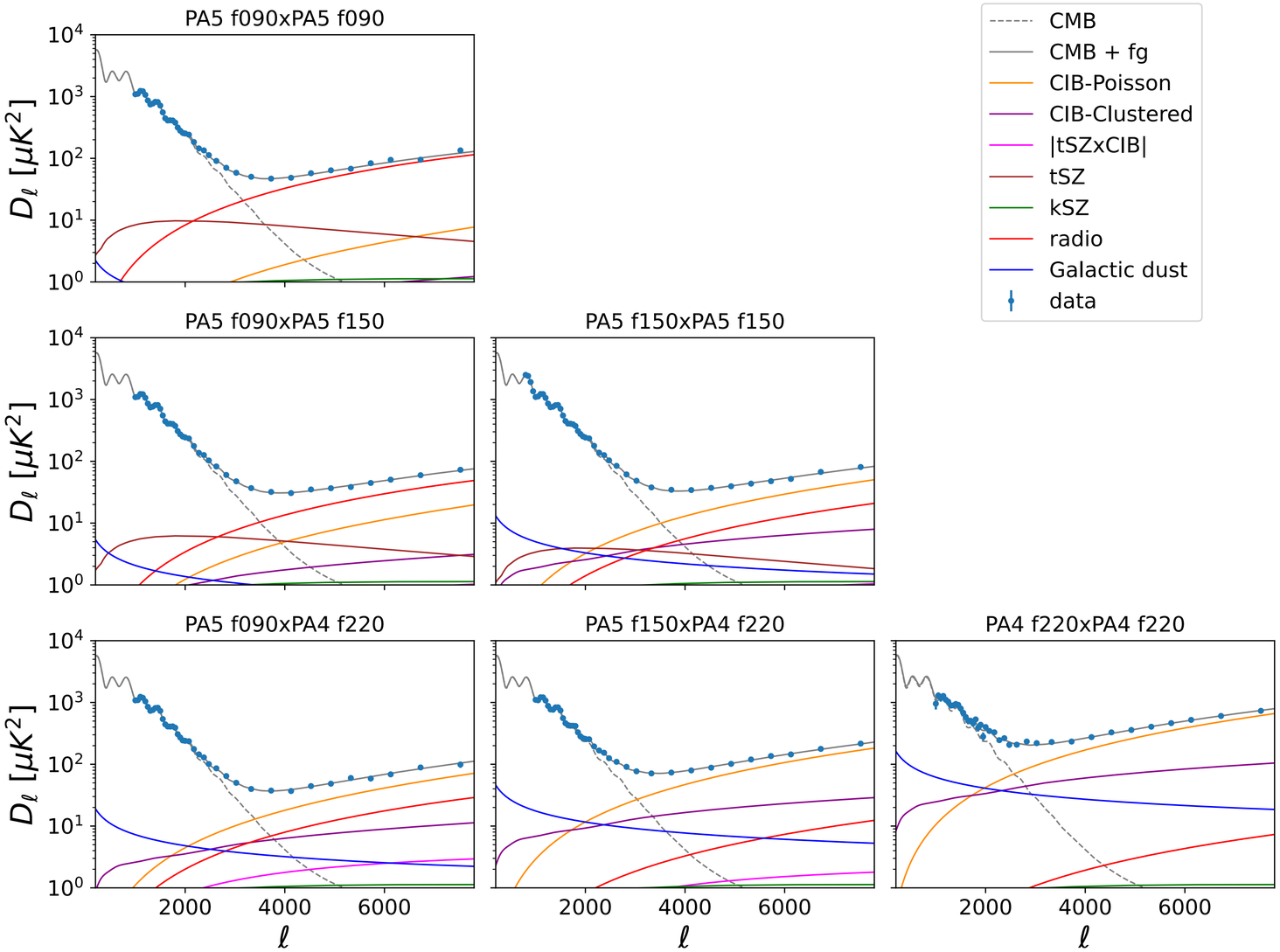

[ACT-DR6 : *Louis et al.* 2503.14452]

ACT-DR6 foreground modelling

- Tested ~20 fg model extensions and assessed the impact on cosmological parameters.
- All changes below 0.1σ.
- No preference for any other model with ACT-DR6 data.

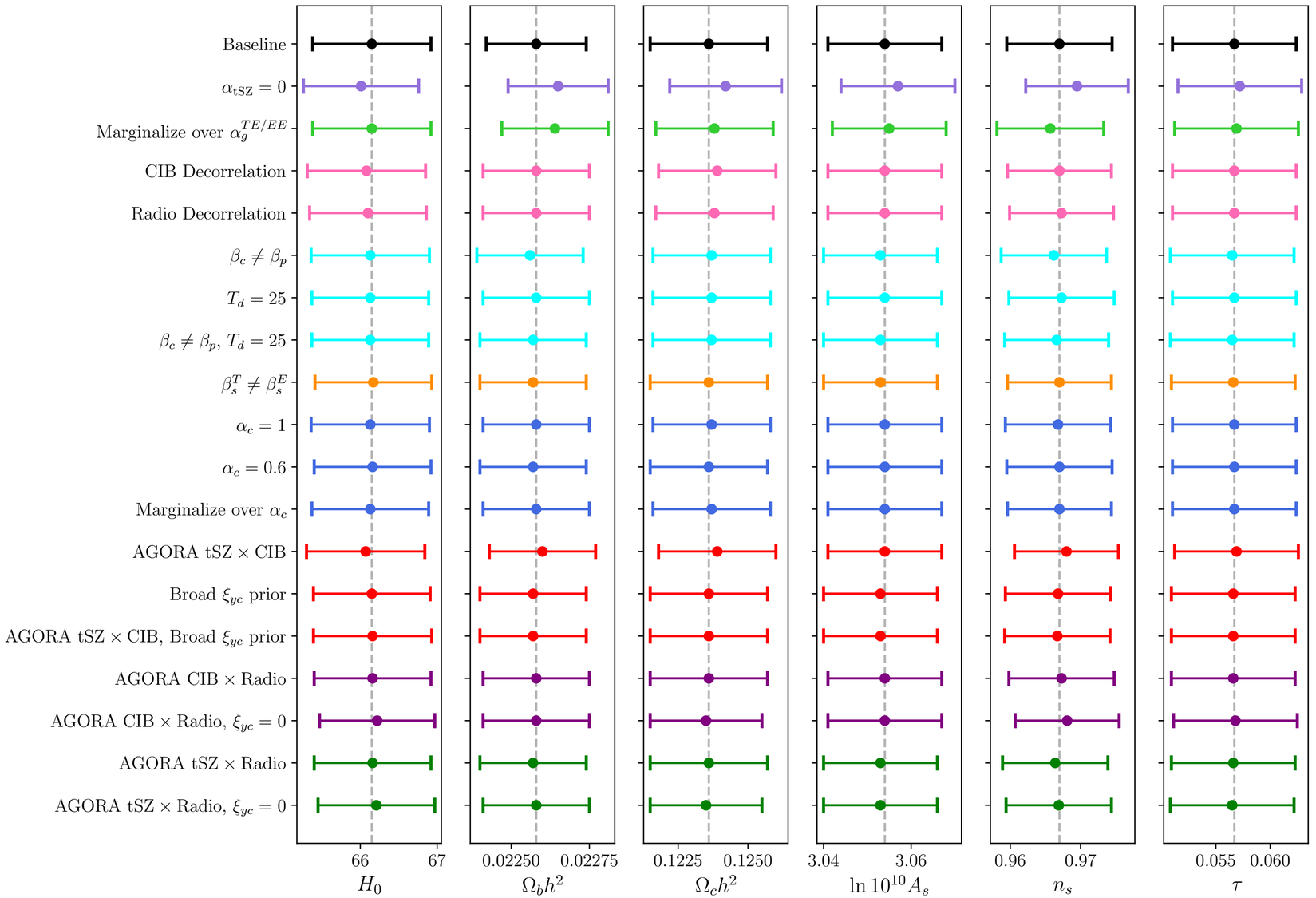

[BB *et al.* 2506.06274]

Modelling of small scales anisotropies - ACT-DR6

$$\mathscr{D}^{T_iT_j}_{\ell,\mathrm{tSZ}} = a_{\mathrm{tSZ}}\mathscr{D}^{\mathrm{tSZ}}_{\ell,\ell_0}\left[\frac{\ell}{\ell_0}\right]^{\alpha_{\mathrm{tSZ}}}\frac{f_{\mathrm{tSZ}}(\nu_i)f_{\mathrm{tSZ}}(\nu_j)}{f^2_{\mathrm{tSZ}}(\nu_0)}$$

- Introduced new parameter : α_{tSZ} that empirically captures the scale dependence of the tSZ signal.
- Proxy for AGN temperature (in AGORA simulations). [Omori 2023].

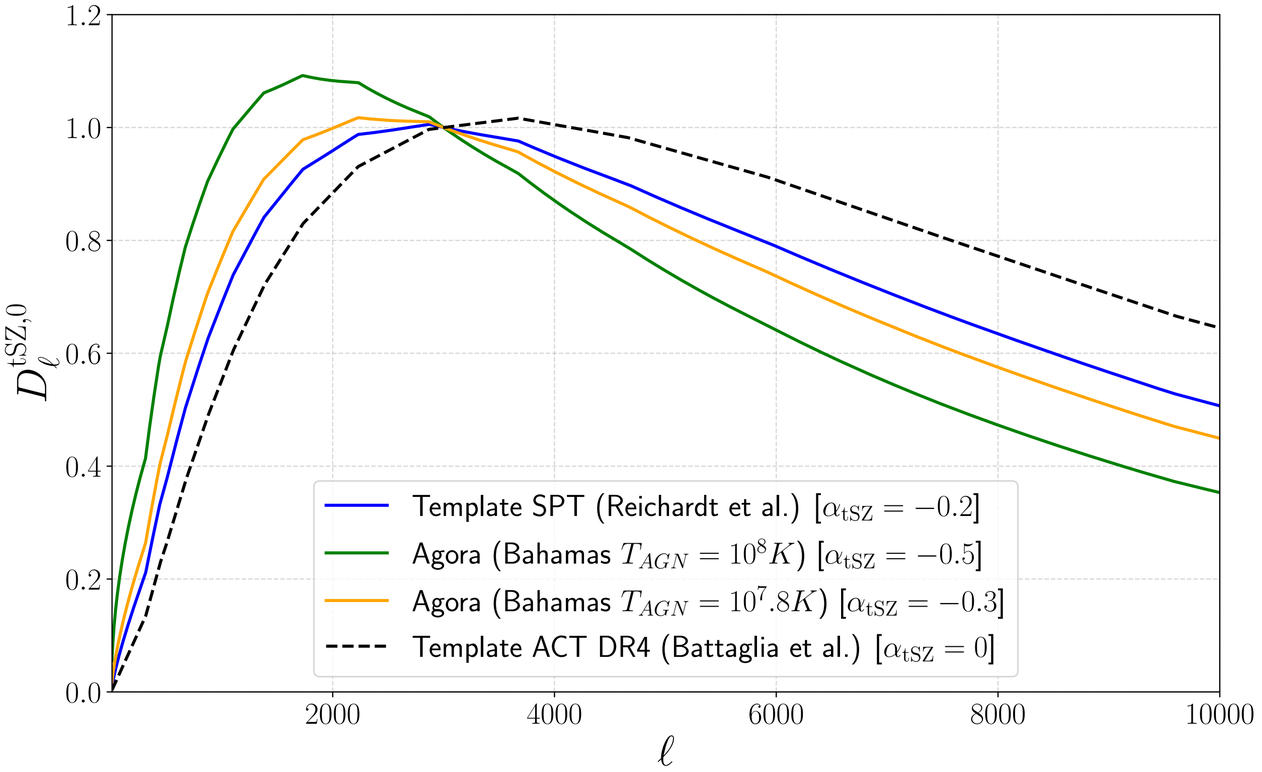

Modelling of small scales anisotropies - ACT-DR6

- $> 0.5\sigma$ shift in cosmological parameters when $\alpha_{\rm tSZ} = 0$.

Parameter	ACT ΛCDM	ACT ΛCDM + $N_{\rm eff}$	P-ACT ΛCDM	P-ACT ΛCDM + $N_{\rm eff}$
H_0	-0.1	-0.3	0.3	-0.4
$\Omega_b h^2$	0.3	0.0	0.6	-0.2
$\Omega_c h^2$	0.2	-0.3	-0.2	-0.5
$\ln 10^{10} A_s$	0.2	0.0	0.3	-0.1
n_s	0.2	-0.2	0.8	-0.2
τ	0.1	0.2	0.3	0.1
$N_{\rm eff}$	–	-0.3	–	-0.5

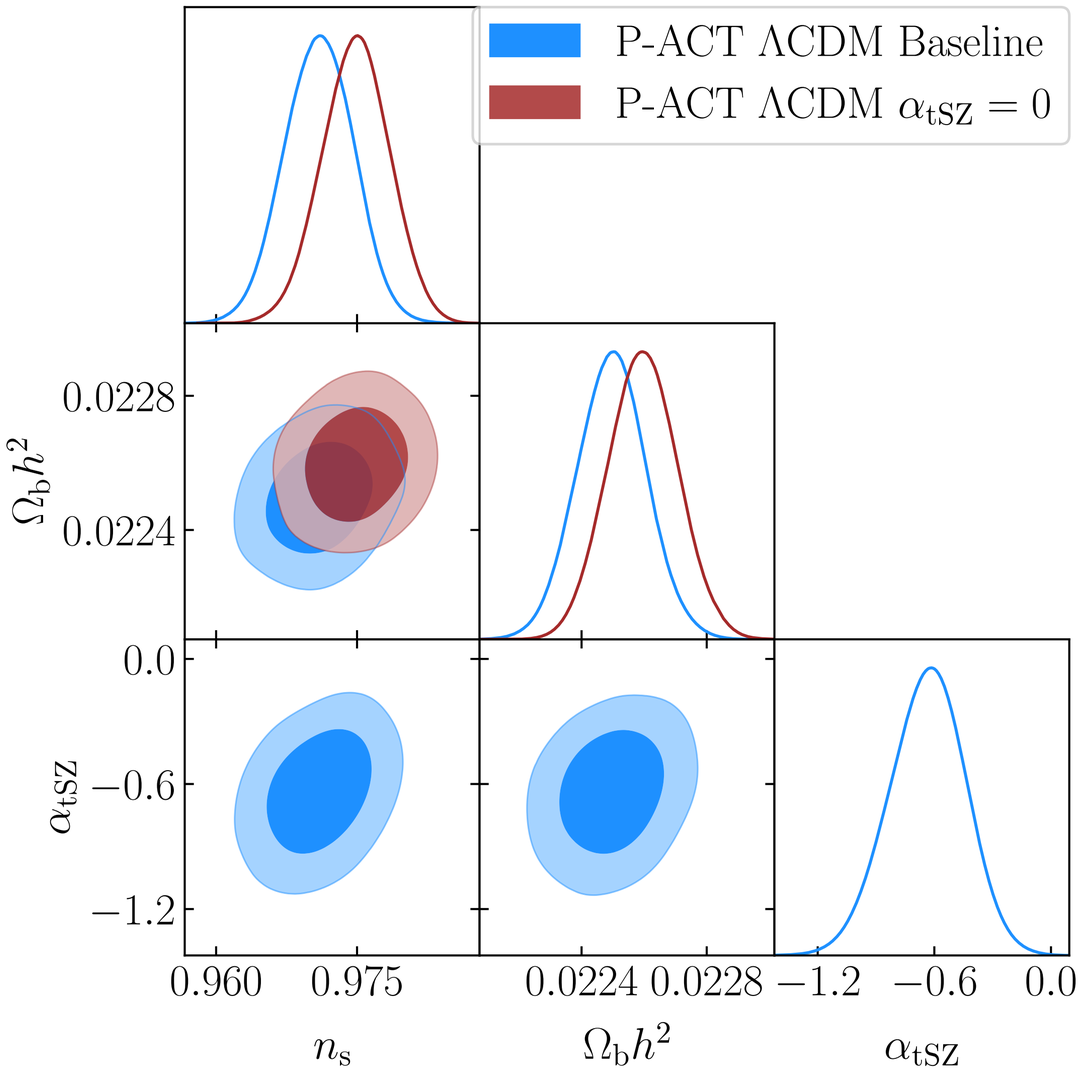

[BB *et al.* 2506.06274]

Outline

- Foreground contamination of CMB observables
- Modelling of small scales temperature and polarisation anistropies
- Component separation methods

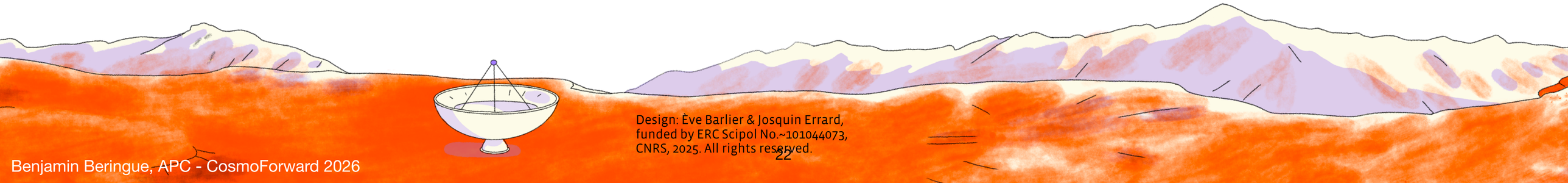

Component separation

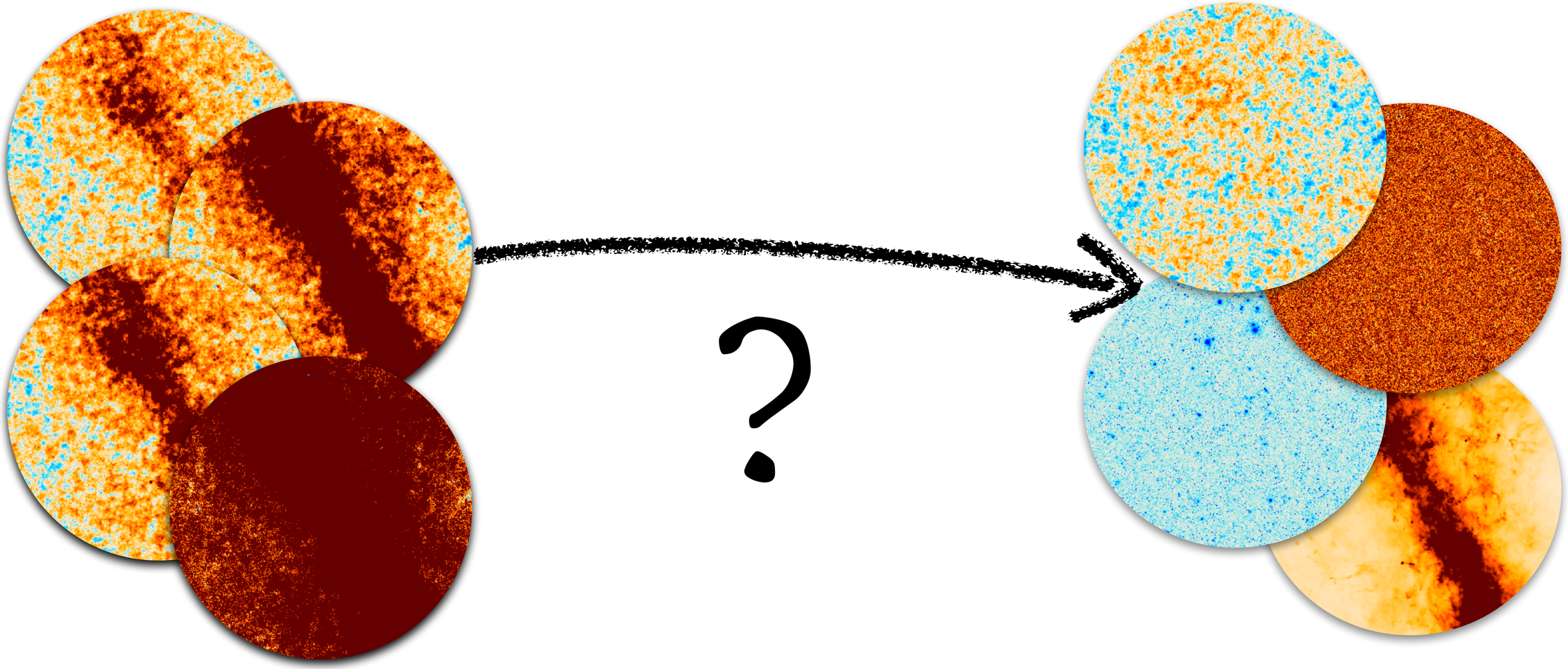

Component separation

$$\mathbf{d} = \mathbf{A} \cdot \mathbf{s} + \mathbf{n}$$

Component separation

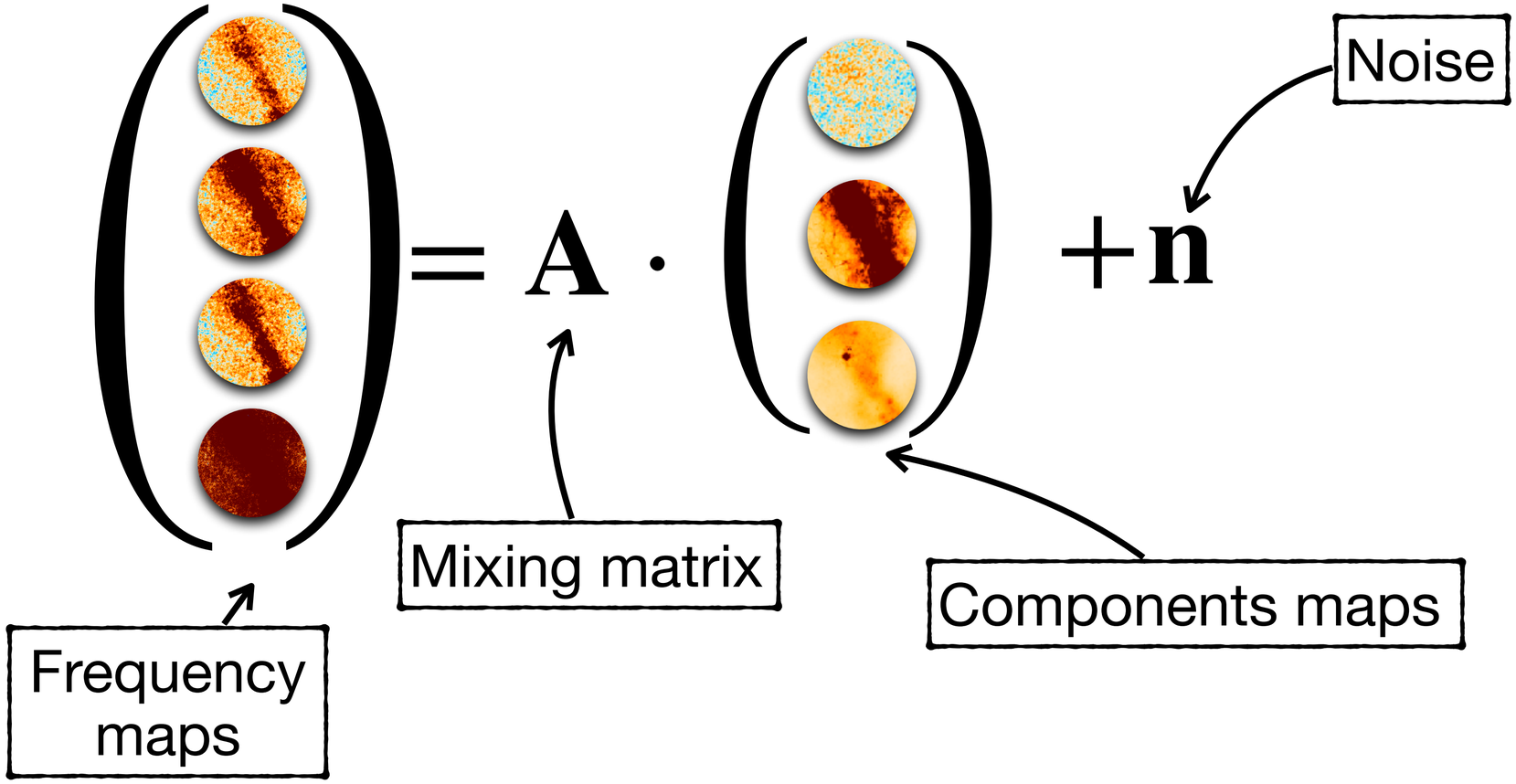

$$\begin{pmatrix} \\ \\ \\ \\ \end{pmatrix} = \mathbf{A} \cdot \begin{pmatrix} \\ \\ \\ \end{pmatrix} + \mathbf{n}$$

Component separation - Internal Linear Combination (ILC)

$$\tilde{\mathbf{s}} = \mathrm{f}(\mathbf{d}) = \mathbf{w} \cdot \mathbf{d}$$

Component separation - Internal Linear Combination (ILC)

$$\tilde{\mathbf{s}} = \mathrm{f}(\mathbf{d}) = \mathbf{w} \cdot \mathbf{d}$$

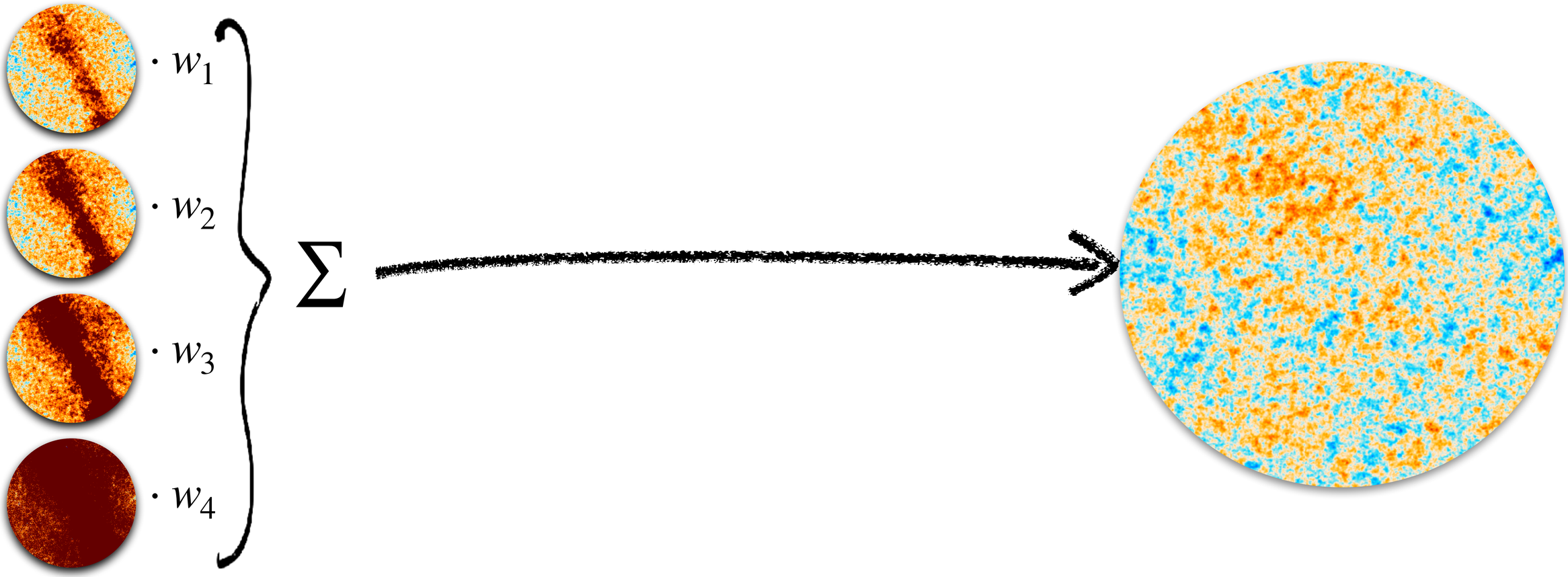

Component separation - Internal Linear Combination (ILC)

$$\tilde{\mathbf{s}} = \mathrm{f}(\mathbf{d}) = \mathbf{w} \cdot \mathbf{d}$$

$\hat{s}_{\mathrm{ILC}}$ has minimum variance.

$\mathbf{w}^{\mathrm{T}} \cdot \mathbf{a} = 1$

$$\mathbf{w}^{\mathrm{T}} = \frac{\mathbf{a}^{\mathrm{T}}\hat{\mathbf{R}}^{-1}}{\mathbf{a}^{\mathrm{T}}\hat{\mathbf{R}}^{-1}\mathbf{a}}$$

Delabrouille et al. 2008

Planck 2018 results. IV, 2020

McCarthy et al. 2024 (pyILC)

…

$$\hat{\mathbf{R}} = \frac{1}{n}\sum \langle \mathbf{d}\mathbf{d}^{\dagger} \rangle$$

Component separation - Internal Linear Combination (ILC)

$$\tilde{\mathbf{s}} = \mathrm{f}(\mathbf{d}) = \mathbf{w} \cdot \mathbf{d}$$

$\hat{s}_{\mathrm{ILC}}$ has minimum variance.

$$\mathbf{w}^{\mathrm{T}} \cdot \mathbf{a} = 1 \qquad \mathbf{w}^{\mathrm{T}} \cdot \mathbf{b} = 0$$

$$\mathbf{w}^{\mathrm{T}} = \frac{\left(\mathbf{b}^{\mathrm{T}}\hat{\mathbf{R}}^{-1}\mathbf{b}\right)\mathbf{a}^{\mathrm{T}}\hat{\mathbf{R}}^{-1} - \left(\mathbf{a}^{\mathrm{T}}\hat{\mathbf{R}}^{-1}\mathbf{b}\right)\mathbf{b}^{\mathrm{T}}\hat{\mathbf{R}}^{-1}}{\left(\mathbf{a}^{\mathrm{T}}\hat{\mathbf{R}}^{-1}\mathbf{a}\right)\left(\mathbf{b}^{\mathrm{T}}\hat{\mathbf{R}}^{-1}\mathbf{b}\right) - \left(\mathbf{a}^{\mathrm{T}}\hat{\mathbf{R}}^{-1}\mathbf{b}\right)^{2}}$$

Delabrouille et al. 2008
Planck 2018 results. IV, 2020
McCarthy et al. 2024 (pyILC)
Remazeilles et al. 2010

$$\hat{\mathbf{R}} = \frac{1}{n}\sum \langle \mathbf{d}\mathbf{d}^{\dagger} \rangle$$

Component separation - Internal Linear Combination (ILC)

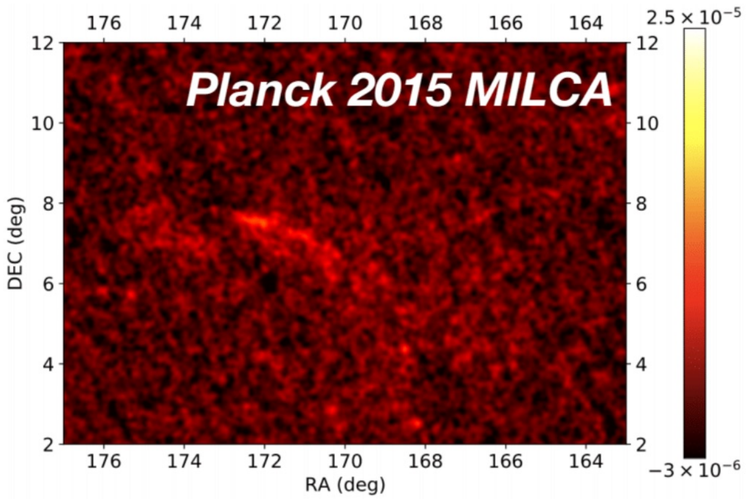

(a) *Planck* MILCA Compton-y map

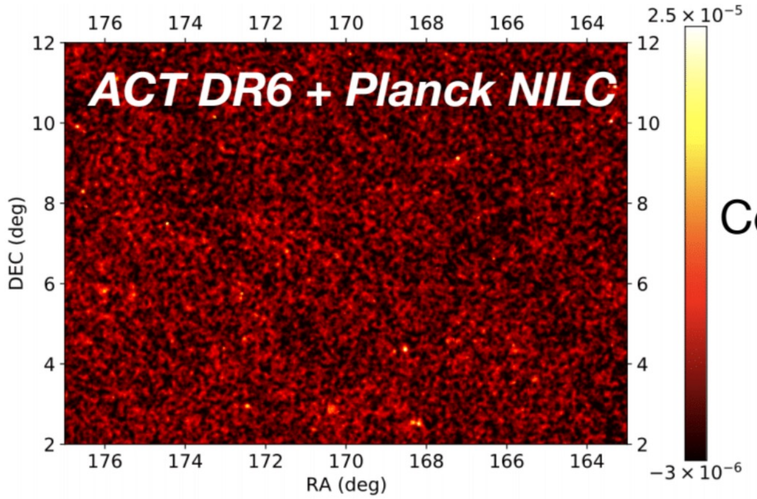

(b) ACT & *Planck* NILC Compton-y map

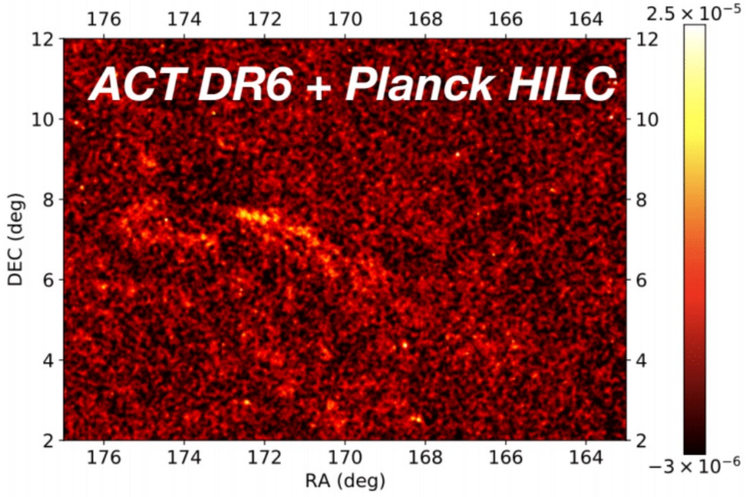

(c) ACT & *Planck* Harmonic ILC Compton-y map

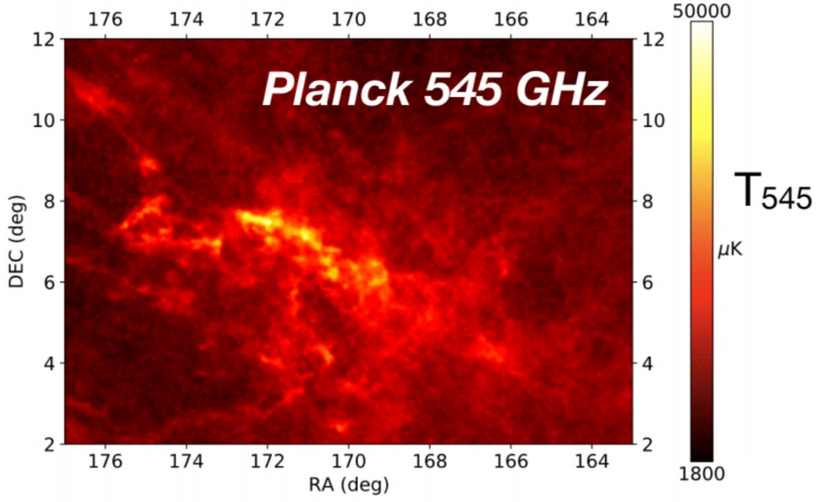

(d) *Planck* 545 GHz map

Coulton et al. (ACT-DR6) (2023)

Component separation - SO-SATs pipelines

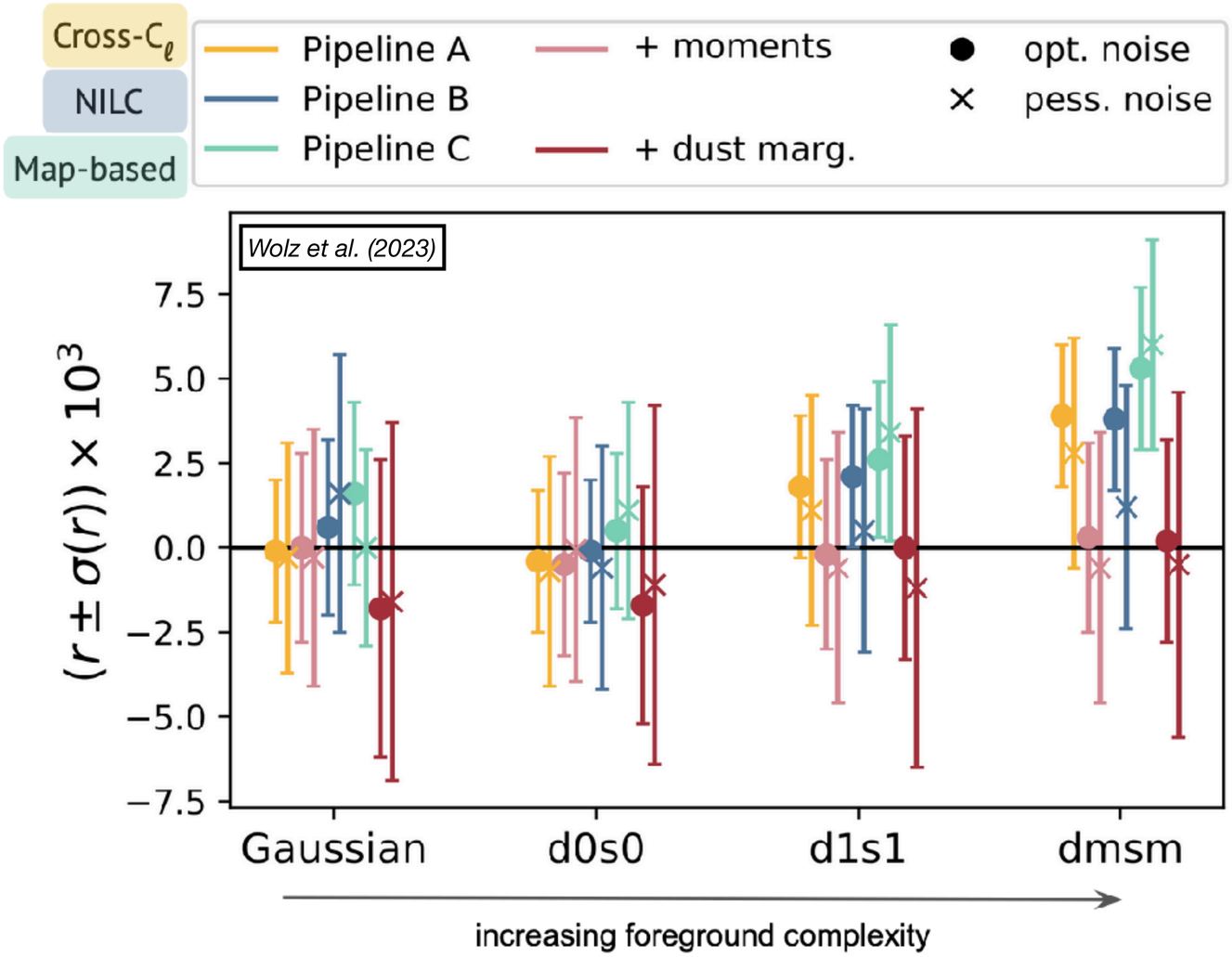

Three main pipelines are developed in SO:

- **Cross-C_ℓ pipeline** (**Soopercool**): multi-frequency, **power spectrum**-based component separation method →baseline BICEP/*Keck*
- **Map-based pipeline** (**Megatop**): multi-frequency, **map**-based component separation method → validated by BICEP/Keck 2018 + Planck reanalysis
- **Needlet-ILC pipeline**: needlet domain internal linear combination methods.

These pipelines combine **parametric and non-parametric** component separation at both map and power spectrum levels, and each addresses **filtering and masking biases** in different ways.

Component separation - SO-SATs pipelines

DATA VECTOR

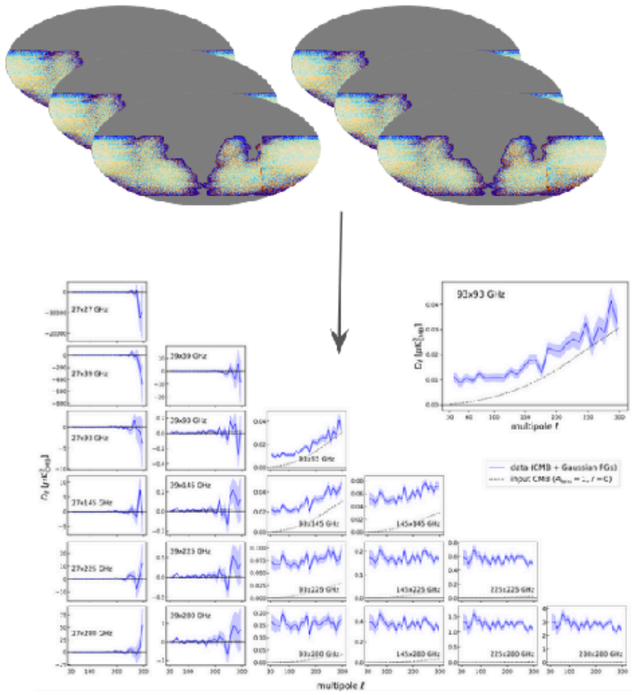

- Full set of **cross-power spectra** between all frequency maps $C_\ell^{\nu\nu'}$;
- Using **data splits** ensures **noiseless** $C_\ell^{\nu\nu'}$ estimates.

Component separation - SO-SATs pipelines

DATA VECTOR

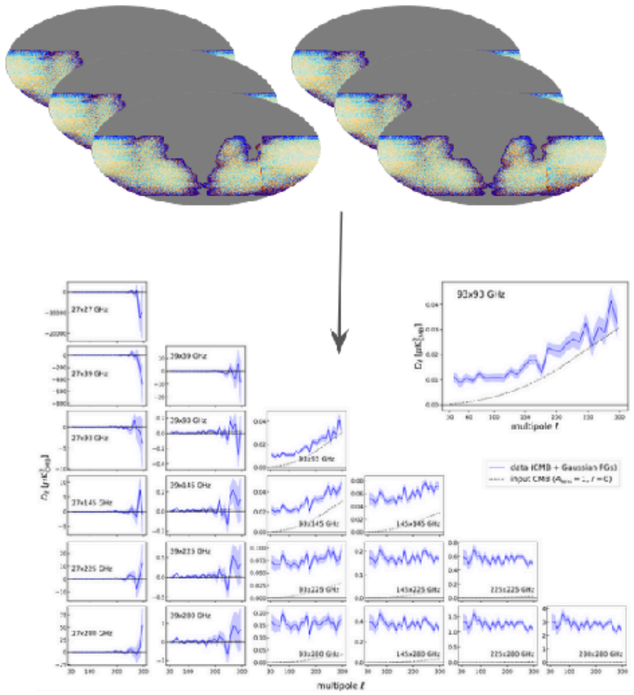

- Full set of **cross-power spectra** between all frequency maps $C_\ell^{\nu\nu'}$;
- Using **data splits** ensures **noiseless** $C_\ell^{\nu\nu'}$ estimates.

MASKING & FILTERING MITIGATION

- Masking & filtering biases accounted for at the power spectrum level:

$$\tilde{C}_b^{\alpha\beta} = \sum_{\ell\gamma\delta} B_{b\ell}^{\alpha\beta,\gamma\delta} C_\ell^{\gamma\delta}$$

$$B_{b\ell}^{\alpha\beta,\gamma\delta} = T_b^{\alpha\beta,\alpha'\beta'} M_{b\ell}^{\alpha'\beta',\gamma\delta}$$

TRANSFER FUNCTION

MODE COUPLING FUNCTION

- **Mode coupling function**: mitigates mask-induced mode coupling;
- **Transfer function:** corrects filtering induced power loss & E→B leakage;
- Both functions estimated through **simulations**.

Component separation - SO-SATs pipelines

DATA VECTOR

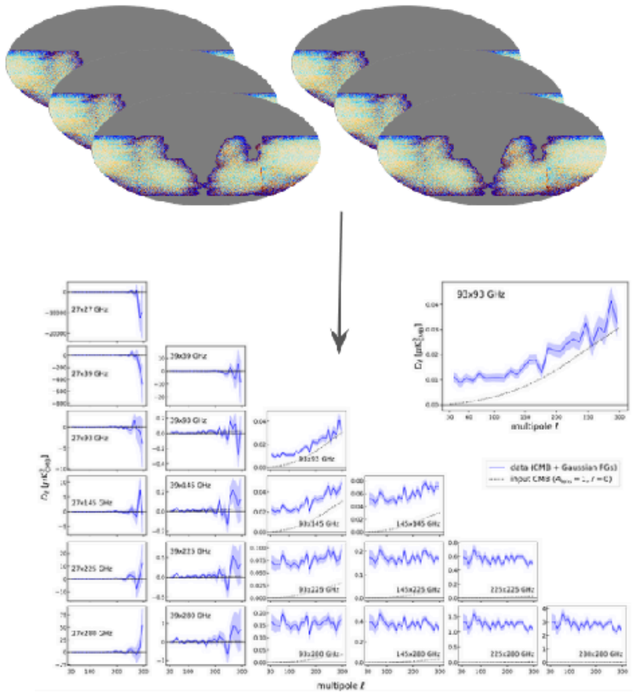

- Full set of **cross-power spectra** between all frequency maps $C_\ell^{\nu\nu'}$;
- Using **data splits** ensures **noiseless** $C_\ell^{\nu\nu'}$ estimates.

MASKING & FILTERING MITIGATION

- Masking & filtering biases accounted for at the power spectrum level:

$$\tilde{C}_b^{\alpha\beta} = \sum_{\ell\gamma\delta} B_{b\ell}^{\alpha\beta,\gamma\delta} C_\ell^{\gamma\delta}$$

$$B_{b\ell}^{\alpha\beta,\gamma\delta} = T_b^{\alpha\beta,\alpha'\beta'} M_{b\ell}^{\alpha'\beta',\gamma\delta}$$

TRANSFER FUNCTION

MODE COUPLING FUNCTION

- **Mode coupling function**: mitigates mask-induced mode coupling;
- **Transfer function:** corrects filtering induced power loss & E→B leakage;
- Both functions estimated through **simulations**.

LIKELIHOOD

- Estimated power spectra compared against a theoretical prediction:

$$-2\ln L(\boldsymbol{\theta}) \approx \sum_\ell (\hat{C}_\ell^{BB} - C_\ell^{BB})^T \hat{\boldsymbol{\Sigma}}_\ell^{-1} (\hat{C}_\ell^{BB} - C_\ell^{BB})$$

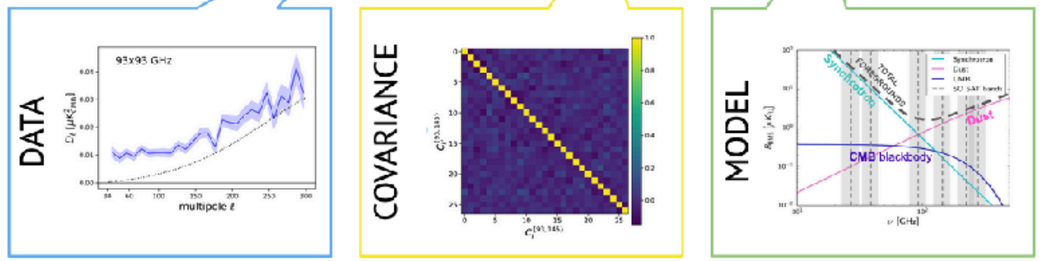

- Relies on **parametric modeling** of foregrounds;
- Requires estimating the **covariance matrix** → from **simulations**.

Component separation - SO-SATs pipelines

DATA VECTOR

$$\mathbf{d}_p = \mathbf{A}(\beta)\mathbf{s}_p + \mathbf{n}_p$$

NOISE

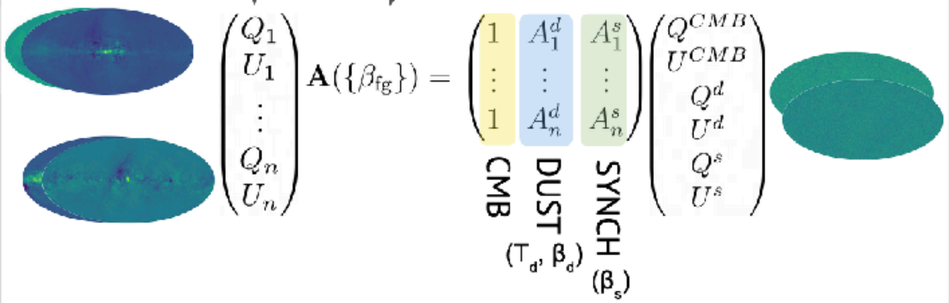

$$\mathbf{A}(\{\beta_{\rm fg}\}) = \begin{pmatrix} 1 & A_1^d & A_1^s \\ \vdots & \vdots & \vdots \\ 1 & A_n^d & A_n^s \end{pmatrix}$$

CMB | DUST (T_d, β_d) | SYNCH (β_s)

$$\begin{pmatrix} Q^{CMB} \\ U^{CMB} \\ Q^d \\ U^d \\ Q^s \\ U^s \end{pmatrix}$$

- Observed **sky signal**: linear combination of **CMB + dust + synchrotron**;
- Combination is encoded in the **mixing matrix A**:
  - Each column → 1 component,
  - Entries → amplitudes of components across frequencies,
  - Depends on **spectral parameters** of foreground emissions,
  - Can include **spatial variations** of parameters [4].

[4] Errard et al. 2019
[5] Stompor et al. 2009
[6] Poletti et al. 2023
[7] Vergès et al. 2021
[8] Jost et al. 2023
[9] Rizzieri et al. 2024
[10] Alonso et al. 2019
[11] Errard et al. 2019


Amalia Villarrubia Aguilar


Maggy Morshed


Baptiste Jost

Component separation - SO-SATs pipelines

DATA VECTOR

$$\mathbf{d}_p = \mathbf{A}(\beta)\mathbf{s}_p + \mathbf{n}_p$$

NOISE

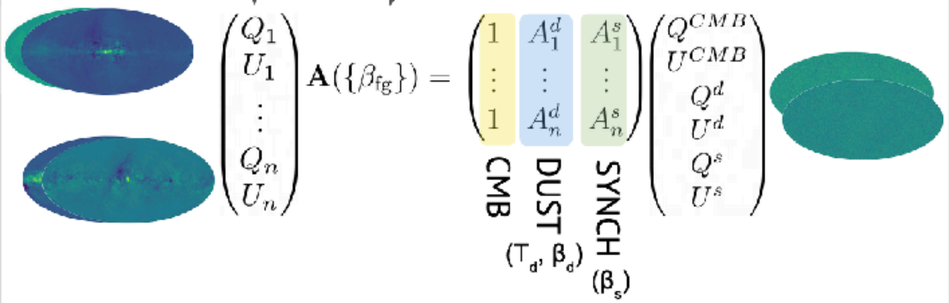

- Observed **sky signal**: linear combination of **CMB + dust + synchrotron**;
- Combination is encoded in the **mixing matrix A**:
  - Each column → 1 component,
  - Entries → amplitudes of components across frequencies,
  - Depends on **spectral parameters** of foreground emissions,
  - Can include **spatial variations** of parameters [4].

COMPONENT SEPARATION

- Map-based component separation is based on the **spectral likelihood** [5], implemented in **FgBuster** [6]:

$$-2\ln\mathcal{L}_{\rm spec}(\beta) = {\rm cst} - \left(\mathbf{A}^t\mathbf{N}^{-1}\mathbf{d}\right)^t \left(\mathbf{A}^t\mathbf{N}^{-1}\mathbf{A}\right)^{-1} \left(\mathbf{A}^t\mathbf{N}^{-1}\mathbf{d}\right)$$

- Relies on the **parametric modelling** of dust & synchrotron:

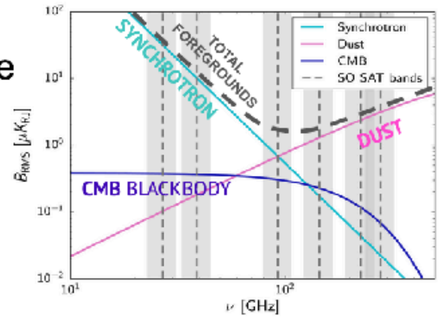

- Extendable to account for **systematic effects**:
  - HWP and bandpass systematics [7],
  - Polarization angle miscalibration [8],
  - Inclusion of main beam [9];
- Outputs **CMB** & **foreground** maps.

[4] Errard et al. 2019
[5] Stompor et al. 2009
[6] Poletti et al. 2023
[7] Vergès et al. 2021
[8] Jost et al. 2023
[9] Rizzieri et al. 2024
[10] Alonso et al. 2019
[11] Errard et al. 2019


Amalia Villarrubia Aguilar


Maggy Morshed


Baptiste Jost

Component separation - SO-SATs pipelines

DATA VECTOR

$$\mathbf{d}_p = \mathbf{A}(\beta)\mathbf{s}_p + \mathbf{n}_p$$

NOISE

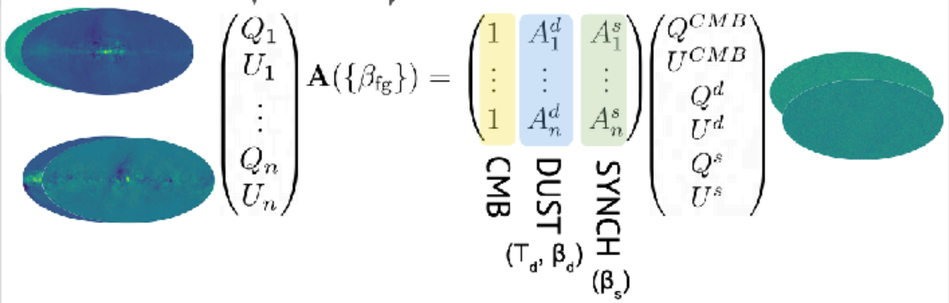

- Observed **sky signal**: linear combination of **CMB + dust + synchrotron**;
- Combination is encoded in the **mixing matrix A**:
  - Each column → 1 component,
  - Entries → amplitudes of components across frequencies,
  - Depends on **spectral parameters** of foreground emissions,
  - Can include **spatial variations** of parameters [4].

COMPONENT SEPARATION

- Map-based component separation is based on the **spectral likelihood** [5], implemented in **FgBuster** [6]:

$$-2\ln\mathcal{L}_{\rm spec}(\beta) = {\rm cst} - \left(\mathbf{A}^t\mathbf{N}^{-1}\mathbf{d}\right)^t \left(\mathbf{A}^t\mathbf{N}^{-1}\mathbf{A}\right)^{-1} \left(\mathbf{A}^t\mathbf{N}^{-1}\mathbf{d}\right)$$

- Relies on the **parametric modelling** of dust & synchrotron:

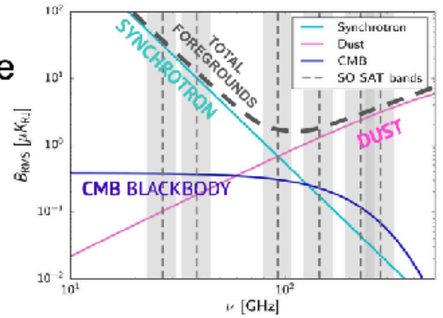

- Extendable to account for **systematic effects**:
  - HWP and bandpass systematics [7],
  - Polarization angle miscalibration [8],
  - Inclusion of main beam [9];
- Outputs **CMB** & **foreground** maps.

COSMOLOGICAL ANALYSIS

- The power spectra estimated using **Namaster** [10];
- The **Cℓs** of the observed CMB map are modeled as:

$$\tilde{C}_\ell^{\rm CMB}(r, A_{\rm lens}) \equiv C_\ell^{\rm prim}(r) + C_\ell^{\rm lens}(A_{\rm lens}) + \tilde{N}_\ell^{\rm CMB}$$

- Cosmological parameters are inferred via the **likelihood:**

$$-2\,\log\mathcal{L}^{\rm cosmo} = \sum_\ell (2\ell+1)\, f_{\rm sky} \left(\frac{\tilde{C}_\ell^{\rm CMB}}{C_\ell^{\rm CMB}} + \log\left(C_\ell^{\rm CMB}\right) \right)$$

- The foreground maps allow for **marginalisation** over the residual dust spectra by extending the model [11]:

$$\tilde{C}_\ell^{\rm CMB} = \tilde{C}_\ell^{\rm CMB}(r, A_{\rm lens}) + A_{\rm dust}\tilde{C}_\ell^{\rm dust}$$


Amalia Villanubia Aguilar


Maggy Morshed


Baptiste Jost

[4] Errard et al. 2019
[5] Stompor et al. 2009
[6] Poletti et al. 2023
[7] Vergès et al. 2021
[8] Jost et al. 2023
[9] Rizzieri et al. 2024
[10] Alonso et al. 2019
[11] Errard et al. 2019

Component separation - SO-SATs pipelines

OBSERVATION MATRIX (baseline)

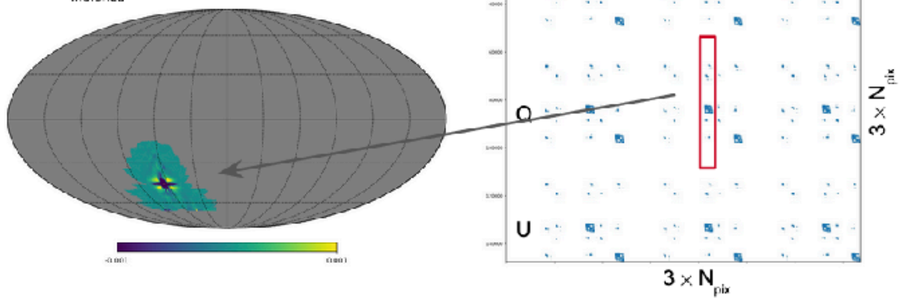

- Filtering in **map space → linear** operation represented by the **observation matrix O**;
- The observation matrix is a (very!) **large**, **sparse** matrix;
- Constructed from the **instrument model** & data **preprocessing** scheme.

- The observation matrix can be included in the **data model** and the **spectral likelihood** to be accounted for during **component separation**:

$$d^{\rm filt.} = \mathcal{O} \cdot d^{\rm raw} = \mathcal{O}A \cdot s + n$$

$$-2\mathcal{L}_{\rm spec.} \sim (A^t\mathcal{O}^t N^{-1} d)^t (A^t\mathcal{O}^t N^{-1}\mathcal{O}A)^{-1} (A^t\mathcal{O}^t N^{-1} d)$$

- The inversion of the central term is costly and requires **efficient computational methods** for feasibility.

PROS
- No need for **simulations**
- Better suited for **pixel-based** analysis
- Describes filtering **spatial variability** and **correlations**

CONS
- High **computational cost**
- Observations matrices need to be available

TRANSFER FUNCTIONS (backup)

- Alternative version of the pipeline: mitigation with **transfer functions** (→ cross-C_ℓ pipeline);
- Transfer functions are estimated externally through **simulations**;
- The input **data vector** and the estimated **noise covariance** matrix are then rescaled:

$$\tilde{\mathbf{d}}_{\ell,m} = \bar{\mathbf{T}}_\ell^{-1/2} \mathbf{d}_{\ell,m}$$

$$\tilde{\mathbf{N}}_\ell = \mathbf{T}_\ell^{-1} \mathbf{N}_\ell$$

- Standard map-based component separation is then performed.

Conclusion

- Still heavily rely on modelling of the foregrounds !
- Large scales polarisation are the most affected by foreground modelling errors.
- Interplay with instrumental systematics is vastly unexplored.
- Need to build models informed by astrophysics.

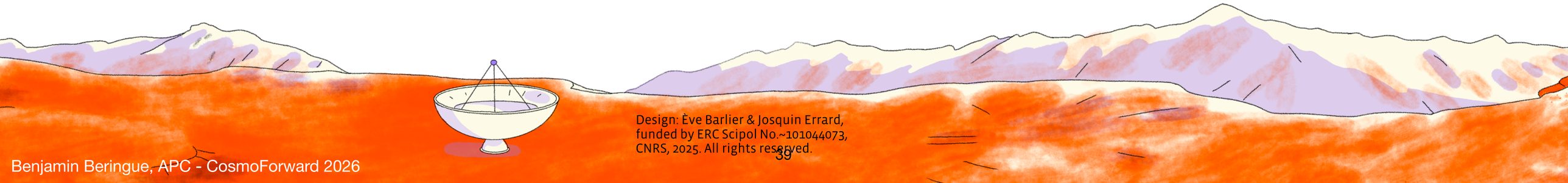

Credit : ESA and the *Planck* Collaboration

Thanks a lot !

beringue@apc.in2p3.fr
beringueb

Science from the large scale cosmic microwave background polarization structure

Constraints on tSZ spectrum

- $\alpha_{\rm tSZ}$ detected at 3σ in P-ACT: $\alpha_{\rm tSZ} = -0.6 \pm 0.2$.
- Higher AGN temperature than expected from AGORA/BAHAMAS simulations.
- Show sensitivity of multi-frequencies CMB data to tSZ modelling.

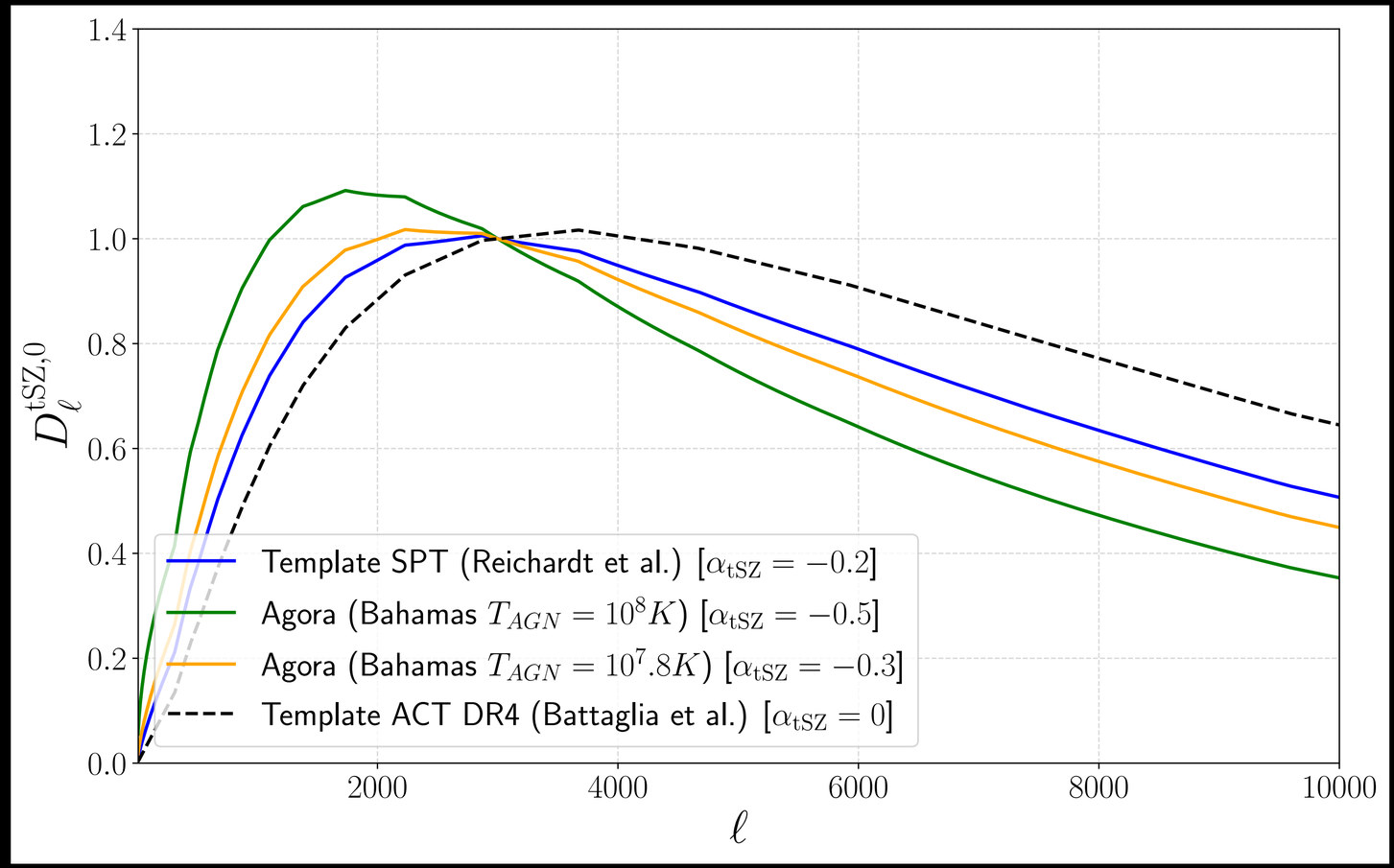

Constraints on tSZ spectrum

- $\alpha_{\rm tSZ}$ detected at 3σ in P-ACT: $\alpha_{\rm tSZ} = -0.6 \pm 0.2$.
- Higher AGN temperature than expected from AGORA/BAHAMAS simulations.
- Show sensitivity of multi-frequencies CMB data to tSZ modelling.

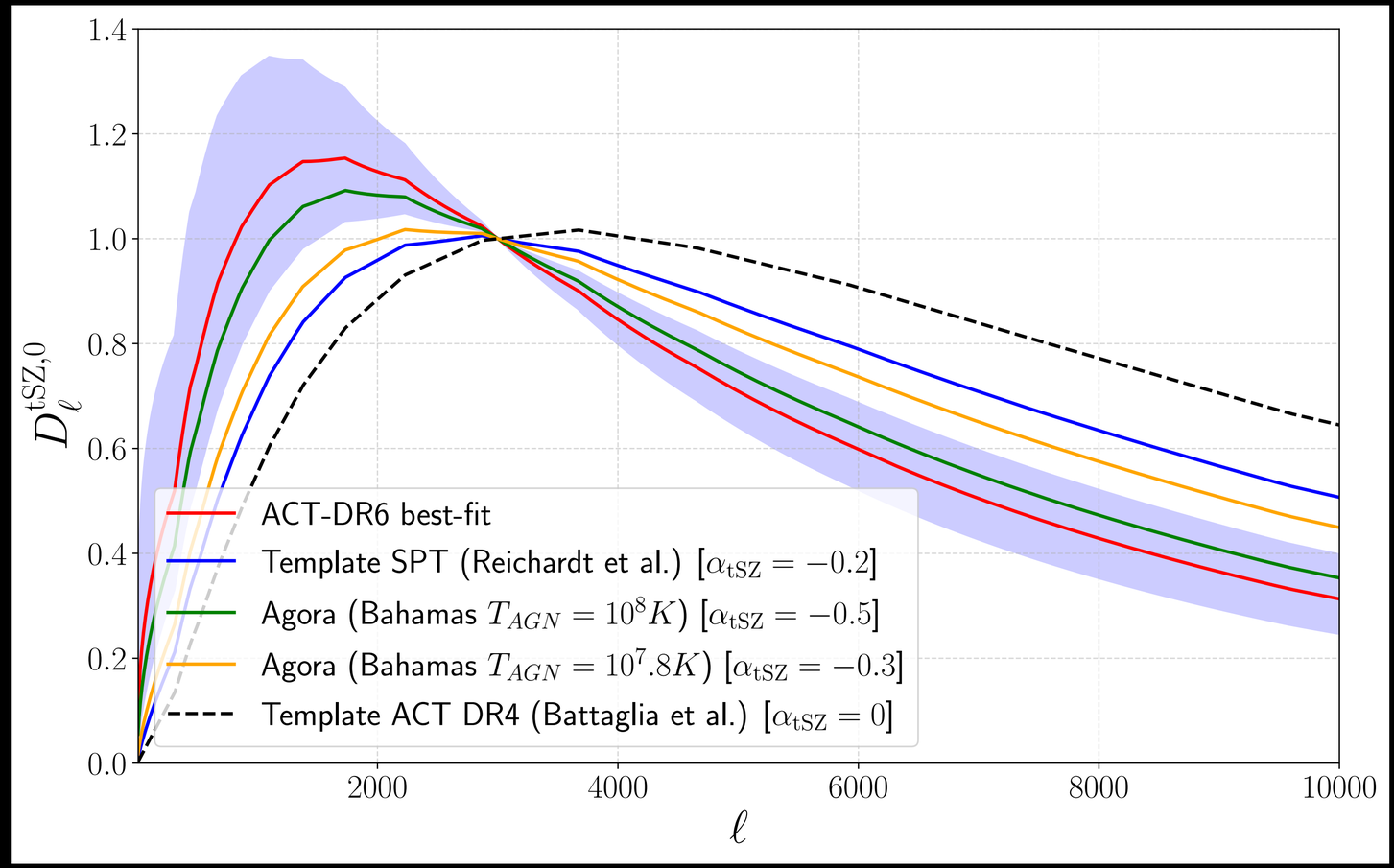

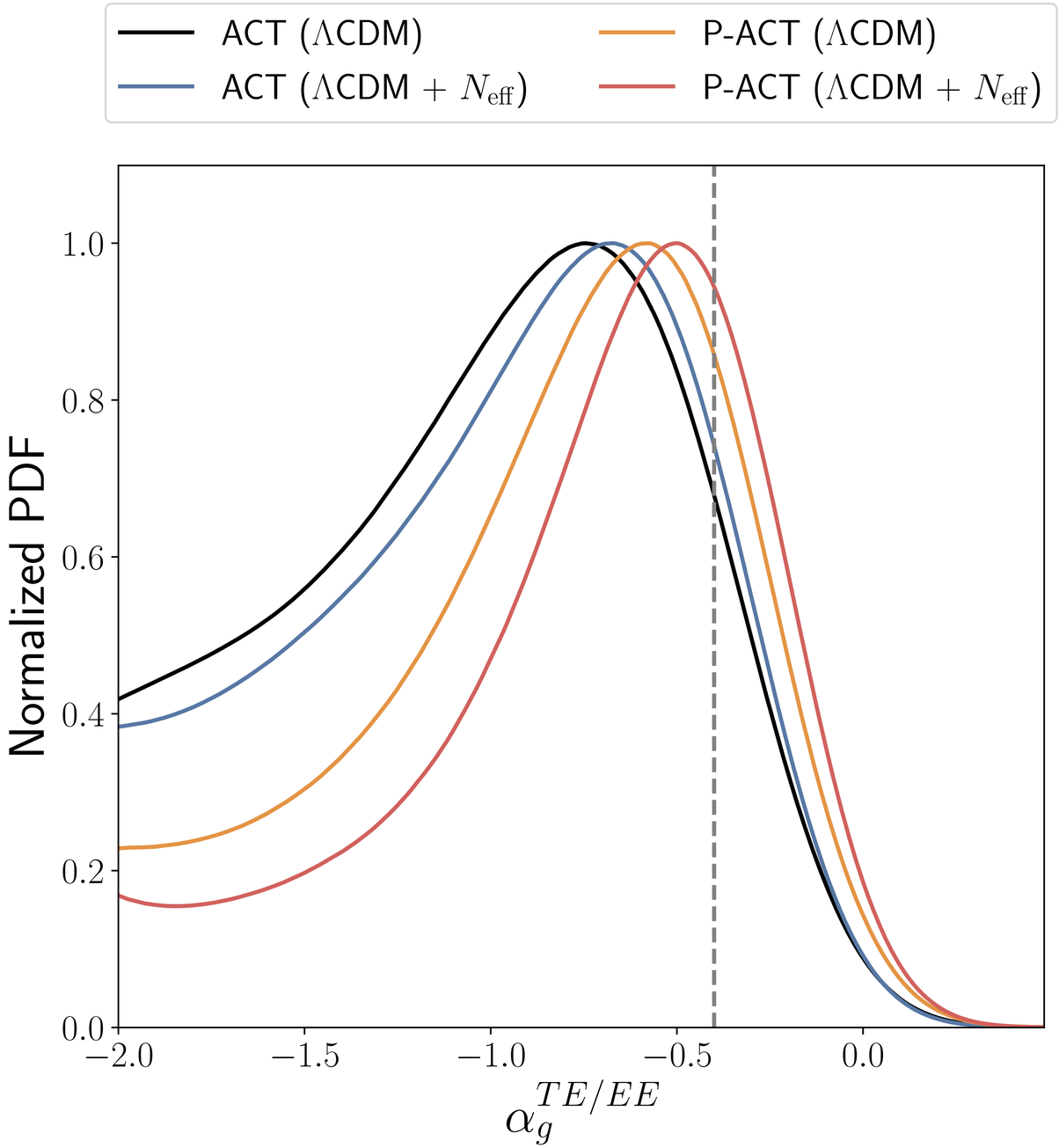
ACT (ΛCDM)
ACT (ΛCDM + $N_{\rm eff}$)
P-ACT (ΛCDM)
P-ACT (ΛCDM + $N_{\rm eff}$)
Normalized PDF
1.0
0.8
0.6
0.4
0.2
0.0
−2.0
−1.5
−1.0
−0.5
0.0
$\alpha_g^{TE/EE}$

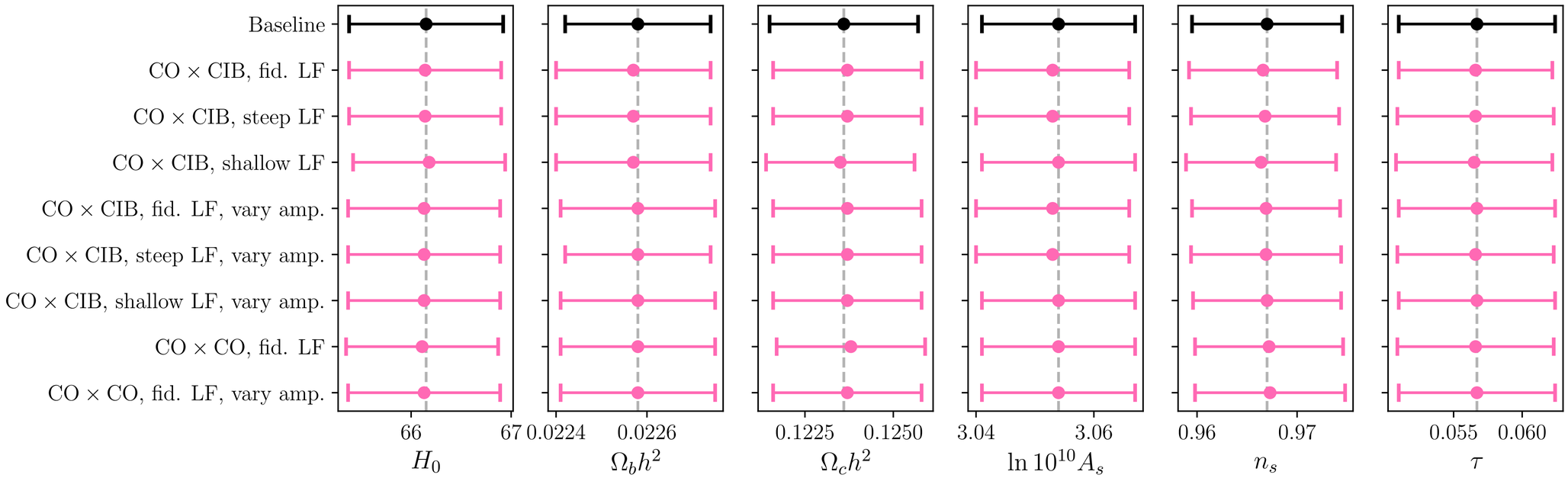
Baseline
CO × CIB, fid. LF
CO × CIB, steep LF
CO × CIB, shallow LF
CO × CIB, fid. LF, vary amp.
CO × CIB, steep LF, vary amp.
CO × CIB, shallow LF, vary amp.
CO × CO, fid. LF
CO × CO, fid. LF, vary amp.
66
67
H_0
0.0224
0.0226
$\Omega_b h^2$
0.1225
0.1250
$\Omega_c h^2$
3.04
3.06
$\ln 10^{10} A_s$
0.96
0.97
n_s
0.055
0.060
τ

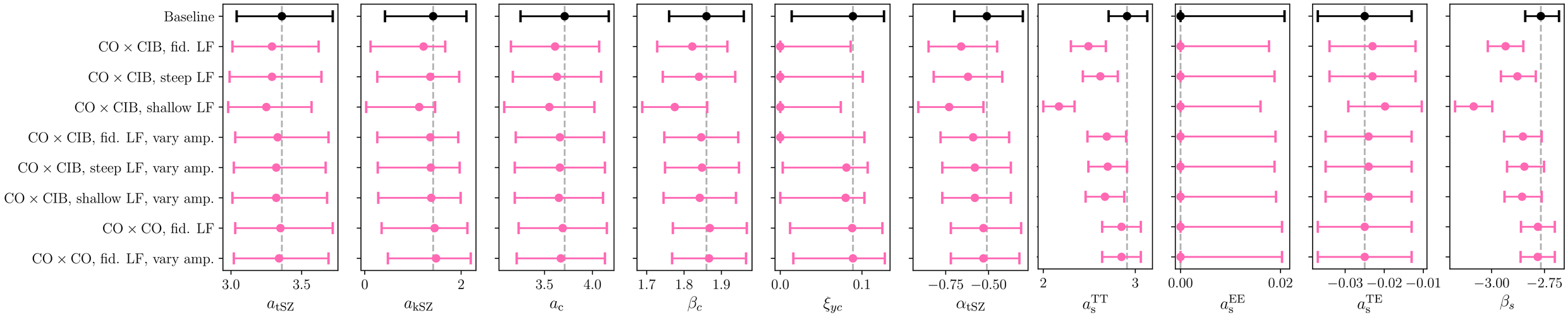
Baseline
CO × CIB, fid. LF
CO × CIB, steep LF
CO × CIB, shallow LF
CO × CIB, fid. LF, vary amp.
CO × CIB, steep LF, vary amp.
CO × CIB, shallow LF, vary amp.
CO × CO, fid. LF
CO × CO, fid. LF, vary amp.
3.0
3.5
$a_{\rm tSZ}$
0
2
$a_{\rm kSZ}$
3.5
4.0
$a_{\rm c}$
1.7
1.8
1.9
β_c
0.0
0.1
ξ_{yc}
−0.75
−0.50
$\alpha_{\rm tSZ}$
2
3
$a_{\rm s}^{\rm TT}$
0.00
0.02
$a_{\rm s}^{\rm EE}$
−0.03
−0.02
−0.01
$a_{\rm s}^{\rm TE}$
−3.00
−2.75
β_s

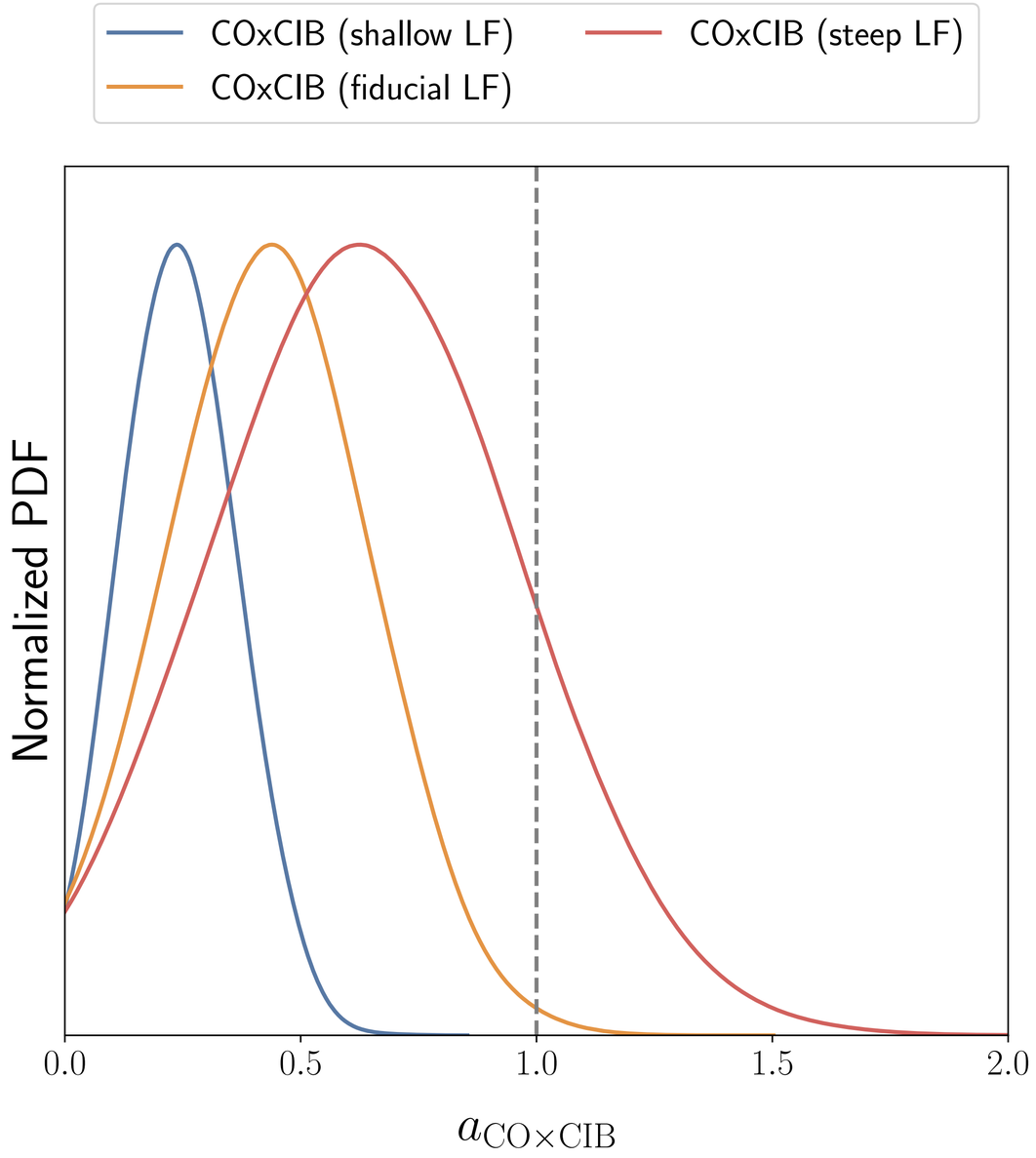
COxCIB (shallow LF)
COxCIB (steep LF)
COxCIB (fiducial LF)
Normalized PDF
0.0
0.5
1.0
1.5
2.0
$a_{\mathrm{CO}\times\mathrm{CIB}}$


Baseline
$\alpha_{\rm tSZ} = 0$
Marginalize over $\alpha_g^{TE/EE}$
CIB Decorrelation
Radio Decorrelation
$\beta_c \neq \beta_p$
$\beta_s^T \neq \beta_s^E$
Marginalize over α_c
AGORA CIB × Radio
AGORA tSZ × Radio
62.5 65.0
H_0
0.0222 0.0225
$\Omega_b h^2$
0.11 0.12
$\Omega_c h^2$
3.025 3.050
$\ln 10^{10} A_s$
0.925 0.950
n_s
0.050 0.055
τ
2.25 2.50 2.75
$N_{\rm eff}$
3 4
$a_{\rm tSZ}$
0 2
$a_{\rm kSZ}$
7 8
$a_{\rm p}$
2 4
a_c
2 3
β_c
−0.75 −0.50 −0.25
$\alpha_{\rm tSZ}$
0.0 0.2
ξ_{yc}
2.5 3.0
$a_{\rm s}^{\rm TT}$
0.00 0.02
$a_{\rm s}^{\rm EE}$
−0.04 −0.02
$a_{\rm s}^{\rm TE}$
−2.9 −2.8 −2.7
β_s